



HAL
open science

Bacterial peptidoglycan serves as a critical modulator of the gut-immune-brain axis in *Drosophila*

Florent Fioriti, Aline Rifflet, Ivo Gomperts Boneca, Olivier Zugasti, Julien Royet

► To cite this version:

Florent Fioriti, Aline Rifflet, Ivo Gomperts Boneca, Olivier Zugasti, Julien Royet. Bacterial peptidoglycan serves as a critical modulator of the gut-immune-brain axis in *Drosophila*. *Brain, Behavior, and Immunity*, 2024, 119, pp.878 - 897. 10.1016/j.bbi.2024.05.009 . pasteur-04614803

HAL Id: pasteur-04614803

<https://pasteur.hal.science/pasteur-04614803>

Submitted on 17 Jun 2024

HAL is a multi-disciplinary open access archive for the deposit and dissemination of scientific research documents, whether they are published or not. The documents may come from teaching and research institutions in France or abroad, or from public or private research centers.

L'archive ouverte pluridisciplinaire **HAL**, est destinée au dépôt et à la diffusion de documents scientifiques de niveau recherche, publiés ou non, émanant des établissements d'enseignement et de recherche français ou étrangers, des laboratoires publics ou privés.



Distributed under a Creative Commons Attribution 4.0 International License



Bacterial peptidoglycan serves as a critical modulator of the gut-immune-brain axis in *Drosophila*

Florent Fioriti^a, Aline Rifflet^b, Ivo Gomperts Boneca^b, Olivier Zugasti^{a,1,*}, Julien Royet^{a,1,*}

^a Institut de Biologie du Développement de Marseille, Aix-Marseille Université, CNRS UMR 7288 Marseille, France

^b Institut Pasteur, Université Paris Cité, CNRS UMR6047, INSERM U1306, 75015 Paris, France

ARTICLE INFO

Keywords:

Drosophila
Gut-brain axis
Peptidoglycan
NF-κB

ABSTRACT

Metabolites and compounds derived from gut-associated bacteria can modulate numerous physiological processes in the host, including immunity and behavior. Using a model of oral bacterial infection, we previously demonstrated that gut-derived peptidoglycan (PGN), an essential constituent of the bacterial cell envelope, influences female fruit fly egg-laying behavior by activating the NF-κB cascade in a subset of brain neurons. These findings underscore PGN as a potential mediator of communication between gut bacteria and the brain in *Drosophila*, prompting further investigation into its impact on all brain cells. Through high-resolution mass spectrometry, we now show that PGN fragments produced by gut bacteria can rapidly reach the central nervous system. In addition, by employing a combination of whole-genome transcriptome analyses, comprehensive genetic assays, and reporter gene systems, we reveal that gut bacterial infection triggers a PGN dose-dependent NF-κB immune response in perineurial glia, forming the continuous outer cell layer of the blood–brain barrier. Furthermore, we demonstrate that persistent PGN-dependent NF-κB activation in perineurial glial cells correlates with a reduction in lifespan and early neurological decline. Overall, our findings establish gut-derived PGN as a critical mediator of the gut-immune-brain axis in *Drosophila*.

1. Introduction

Organisms with an open digestive system have in common the colonization of the gastrointestinal tract by various species of microorganisms, of which bacteria make up the largest proportion, along with yeasts and viruses (McFall-Ngai et al., 2013; Proctor et al., 2019). This community of micro-organisms, known as the gut microbiota, feeds on nutrients generated by the host's diet and is influenced by host-specific factors, including the gut environment and food preferences (Moszak et al., 2020). In turn, gut micro-organisms intricately interact with the host by producing and releasing microbiota-derived products and metabolites that impact on many physiological processes, including metabolism, immune responses, and even the functioning of the host brain (Agus et al., 2021; Morais et al., 2021; Nagpal and Cryan, 2021). These interactions play a pivotal role in maintaining the homeostasis and therefore the health of the organism (Fan and Pedersen, 2021; Kamareddine et al., 2020).

Among the products derived from the microbiota that ensure communication with the host, microbe- and pathogen-associated

molecular patterns (MAMPs/PAMPs) represent conserved molecules that play an important role in modulating the host immune response, helping to maintain a balance between tolerance and defense against pathogens (Janeway and Medzhitov, 2002; Kawai and Akira, 2009). One of these MAMPs is peptidoglycan (PGN), also known as murein, an essential structural component of the cell wall of most bacteria (Schleifer and Kandler, 1972; Wolf and Underhill, 2018). Made up of long disaccharide chains that are linked by peptide bridges, PGN forms a mesh-like layer outside the bacterial plasma membrane (Vollmer et al., 2008). In eukaryotes, circulating fragments of PGN released during bacterial growth or cell death, known as muropeptides, are detected by several families of Pattern Recognition Receptors (PRRs) either intracellularly or at the cell membrane (Irazoki et al., 2019; Park and Uehara, 2008). These include Nucleotide-binding Oligomerisation Domain (NOD) proteins in vertebrates, as well as PGN-Binding Proteins (PGRPs) in both vertebrates and invertebrates (Girardin and Philpott, 2004; Myllymäki et al., 2014; Neyen et al., 2012). In response to PGN fragments, PRR activate evolutionary conserved intracellular signaling cascades triggering the nuclear factor-kappa B (NF-κB) family of transcriptional

* Corresponding authors.

E-mail addresses: olivier.zugasti@univ-amu.fr (O. Zugasti), julien.royet@univ-amu.fr (J. Royet).

¹ These authors share last authorship on this work.

regulators, an integral component of the innate immune response responsible for both inflammation and antimicrobial activity (Liu et al., 2017; Myllymäki et al., 2014).

The interactions between PGN fragments produced by intestinal bacteria and the NOD and PGRP receptors expressed by enteric cells are essential to simultaneously eliminate pathogenic gut bacteria while preserving innocuous commensal ones (Biswas and Kobayashi, 2013; Bosco-Drayon et al., 2012; Onuma et al., 2023; Vance et al., 2009). Although, in this case, the interaction between PGN and its dedicated receptors is short-range, it has been demonstrated that by activating its receptors in distant tissues and organs, gut-derived PGN is able to control from a distance biological processes such as the immune response, hematopoiesis and metabolism (Clarke et al., 2010; Sorbara and Philpott, 2011). Studies conducted in humans and various animal models indicate that the influence of PGN and its derived muropeptides extends to the central nervous system (CNS). Pioneering investigations have identified the presence of PGN within human astrocytes, potentially serving as a catalyst for brain inflammation in conditions such as multiple sclerosis and autoimmune encephalomyelitis (Branton et al., 2016; Laman et al., 2020; Visser et al., 2005). In mice, detection of PGN derived from the commensal gut microbiota by PGN-sensing molecules expressed in neurons and astrocytes modulates brain development and social behavior (Arentsen et al., 2017). Furthermore, research has demonstrated that PGN fragments can cross the murine placenta, stimulating the proliferation of neurons in the fetal cortex in a TLR2-dependent manner (Humann et al., 2016). Recent findings also indicate that orally administered Muramyl Dipeptide (MDP) reaches the mouse brain and directly stimulates GABAergic hypothalamic neurons expressing NOD2, thereby modulating feeding behavior, nesting behavior, and body temperature (Gabanyi et al., 2022). Additionally, investigations conducted in our laboratory using the fruit fly *Drosophila melanogaster*, primarily through genetic strategies, have demonstrated that injection of PGN into the body cavity modulates oviposition behavior, leading to a reduction in the number of eggs laid by the flies. This change in behavior appears to be a direct consequence of the activation of the evolutionarily conserved Immune Deficiency/NF- κ B (IMD/NF- κ B) signaling cascade within a subset of octopaminergic neurons (Kurz et al., 2017; Masuzzo et al., 2019). Our results strongly suggest that PGN, when present in the hemolymph, a fluid analogous to the blood in vertebrates, has the potential to come into contact with neural cells and can cross the blood–brain barrier to influence the functions of the fly brain. In this study, we extend our investigation into the role of PGN released by intestinal bacteria as a regulator of gut bacteria–brain interactions in *Drosophila*. We employ spectrometric approaches to directly investigate the dynamics of dissemination of immunogenic PGN fragments from the gut to host tissues using a bacterial gut infection model. Additionally, we integrate comprehensive transcriptomic and genetic approaches to characterize the consequences of the presence of muropeptides in the CNS.

2. Results

2.1. *E. cc¹⁵* releases higher levels of immunogenic muropeptides than *E. c^{MC4100}*

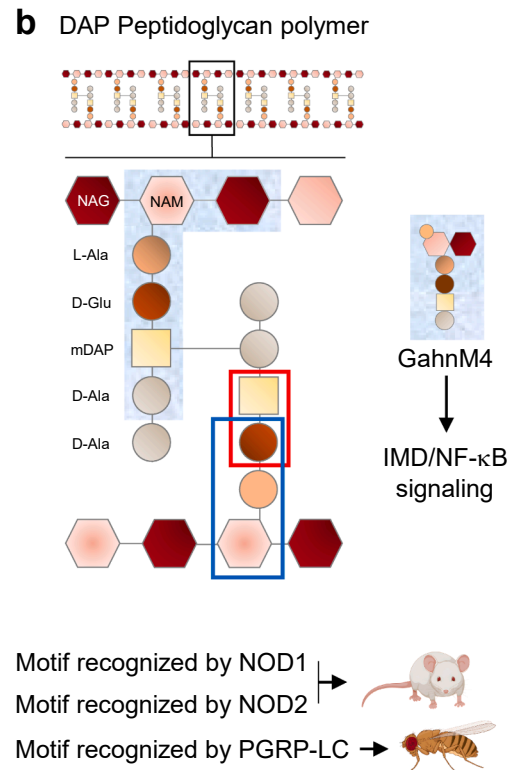
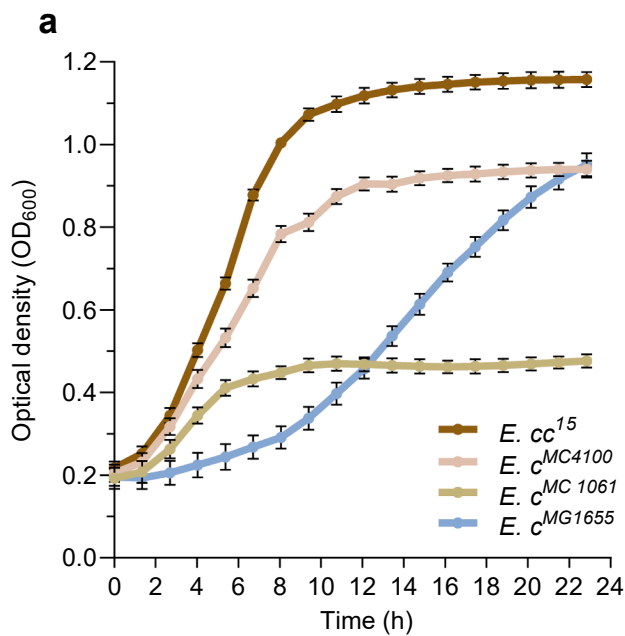
The phytopathogen *Erwinia carotovora carotovora 15* (*E. cc¹⁵*) is a naturally occurring Gram-negative bacterium associated with *Drosophila*, derived from the environment, and extensively utilized to investigate host–bacteria interactions in the fruit fly (Basset et al., 2003; Corby-Harris et al., 2007). It has been reported that, when present in the adult intestinal tract, *E. cc¹⁵* has the ability to activate PGN-dependent innate immune signaling locally and in distant tissues such as the fat body and Malpighian tubules, which are functional equivalents to the mammalian liver and kidneys, respectively, without damaging the integrity of the intestine. (Basset et al., 2000; Buchon et al., 2009; Zugasti et al., 2020). All other bacterial species tested to date appeared

to lack this feature. It is conceivable that the nature and/or the rate of PGN fragments released by *E. cc¹⁵* would explain this rather unique property. To test this hypothesis, we compared the ability of *E. cc¹⁵* and *Escherichia coli MC4100* (*E. c^{MC4100}*), another Gram-negative bacterium sharing comparable growth properties with *E. cc¹⁵* (Fig. 1a), in releasing immunogenic monomeric PGN fragments into the surrounding environment. Although *E. c^{MC4100}* is not naturally associated with *Drosophila*, it can be hosted by the fly and is commonly used to study host–bacteria interactions (Younes et al., 2020). The levels of various monomeric PGN fragments containing γ -D-glutamyl-meso-diaminopimelic acid (iE-DAP) and muramyl dipeptide (MDP), which are the minimal motifs recognized respectively by the intracellular immune receptors NOD1 and NOD2 in mammals (Girardin et al., 2003b, 2003a), along with their anhydro derivatives (Irazoki et al., 2019) (Fig. 1b, c), were quantified in the culture medium of exponentially growing *E. cc¹⁵* and *E. c^{MC4100}* using liquid chromatography–mass spectrometry (LC–MS). While MDP and muramyl tripeptide (GM3) were not found in bacterial supernatants, the muramyl di-, tetra- and pentapeptides (GM2, GM4 and GM5) were identified. Although present at low concentrations, GM2 and GM5 appeared to be ostensibly released to a greater extent by *E. c^{MC4100}*, while GM4 was more abundantly produced by *E. cc¹⁵* (Fig. 1d). On the other hand, anhydromuropeptides were found to be released more abundantly by both *E. cc¹⁵* and *E. c^{MC4100}* in comparison to muropeptides, with significantly higher levels observed in the culture medium of *E. cc¹⁵* compared to *E. c^{MC4100}* (Fig. 1e). Among the anhydromuropeptides, the most abundant was the anhydro-murotetrapeptide (GanhM4), also known as Tracheal cytotoxin (TCT), which has been previously identified as the minimal motif required for activating IMD/NF- κ B signaling in flies (Chang et al., 2006; Kaneko et al., 2004; Lim et al., 2006) (Fig. 1e). These findings demonstrate that *E. cc¹⁵* and *E. c^{MC4100}* preferentially release GanhM4 capable of activating the IMD/NF- κ B pathway, with *E. cc¹⁵* exhibiting higher levels of release.

2.2. *GanhM4* is detected in the gut, the hemolymph and the fat body of *E. cc¹⁵* and *E. c^{MC4100}* fed adult flies

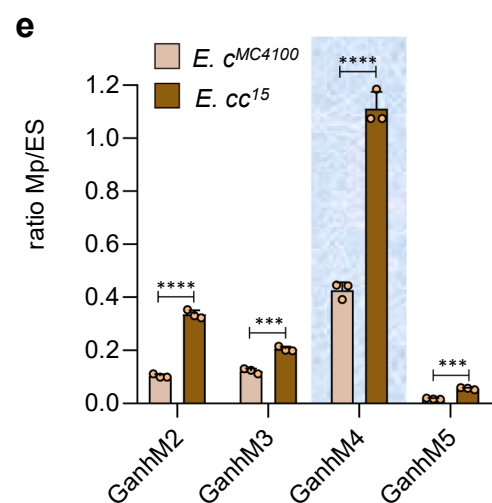
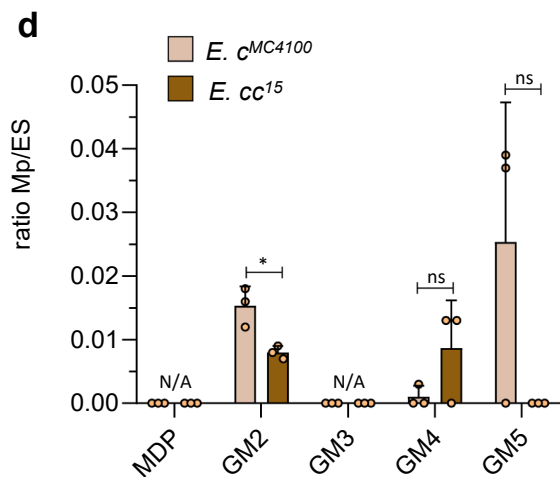
Using the same methodology, we quantified the presence of GanhM4 and its cleaved derivative, the peptide stem AEmDapA, in flies raised on antibiotics and transferred onto a medium contaminated with *E. cc¹⁵* or *E. c^{MC4100}*. Indeed, in order to mitigate the potential adverse effects resulting from excessive or prolonged activation of the NF- κ B pathway, flies, similar to mammals, possess various mechanisms that dampen the level of immunogenic PGN fragments. One of these mechanisms involves the pivotal role played by PGN-cleaving amidases (Buchon et al., 2013). Through the hydrolysis of the amide bond connecting MurNAc to the Ala residue of the stem peptide, catalytic PGRPs, such as PGRP-LB, PGRP-SC1/2, and PGRP-SB1/2, convert the active GanhM4 into the inactive AEmDapA (Bischoff et al., 2006; Charroux et al., 2018; Mellroth and Steiner, 2006; Zaidman-Rémy et al., 2011, 2006) (Fig. S1a). This enzymatic process ultimately reduces the intensity of NF- κ B activation in response to a PGN source (Paredes et al., 2011). Within 30 min following ingestion of either *E. cc¹⁵* or *E. c^{MC4100}*, a significant presence of AEmDapA was detected in extracts from wild-type flies, and its levels remained elevated even 2 h post-infection (Fig. S1b, c). When experiments were conducted in PGRP-LB mutants (PGRP-LB^Δ) both GanhM4 and AEmDapA were detected at the 30 min and 2 h time points post-infection (Fig. S1c). These findings indicate that ligands of the IMD/NF- κ B pathway rapidly translocate into the body cavity following ingestion of either *E. cc¹⁵* or *E. c^{MC4100}* and undergo rapid processing by endogenous amidases.

It is postulated that muropeptides released by gut bacteria traverse the intestinal epithelium to access the hemolymph, analogous to vertebrate blood, which bathes most tissues and organs (Gendrin et al., 2009). Therefore, we conducted an analysis of the local and distant distribution of GanhM4 and AEmDapA in isolated gut and fat body tissues, as well as in the hemolymph. In wild type animals, shortly after oral ingestion of *E.*



c

PGN fragment	Structure	Anhydro-PGN fragment	Structure
Muramyl dipeptide (MDP)		Anhydro-murotdipeptide (GanhM2)	
Murodipeptide (GM2)		Anhydro-murotripeptide (GanhM3)	
Murotripeptide (GM3)		Anhydro-murotetrapeptide (GanhM4)	
Murotetrapeptide (GM4)		Anhydro-muropentapeptide (GanhM5)	
Muropentapeptide (GM5)			



(caption on next page)

Fig. 1. Characterization of muropeptide release by *Erwinia carotovora carotovora* 15 and *Escherichia coli* MC4100. **(a)** Growth curves of *Erwinia carotovora carotovora* (*E. cc*¹⁵) and *Escherichia coli* (*E. c*) strains MC4100, MC1061, and MG1655. **(b)** Schematic representation of peptidoglycan (PGN) polymer and basic structure of peptidoglycan motifs recognized by NOD1/2 and PGRP-LC pattern recognition receptors (PRRs). Abbreviations: L-Ala: L-alanine; D-Glu: D-glutamic acid; D-Ala: D-alanine; mDAP: meso-diaminopimelic acid; NAM: N-acetylmuramic acid; NAG: N-acetylglucosamine. **(c)** Schematic drawing illustrating the structure of monomeric muropeptides and anhydromuropeptides. **(d-e)** Quantification of monomeric muropeptides (MDP, GM2, GM3, GM4, GM5) **(d)** and anhydromuropeptides (GanhM2, GanhM3, GanhM4, GanhM5) **(e)** released by *E. cc*¹⁵ and *E. c*^{MC4100}, as determined by liquid chromatography-mass spectrometry (LC-MS). Ratios of each muropeptide to the external standard (ES) are presented on the Y-axis. Comparisons between selected conditions in **(d)** and **(e)** are shown (unpaired *t*-test, ns = not significant, *****p* < 0.0001, ****p* < 0.001, ***p* < 0.01, and **p* < 0.1).

*cc*¹⁵ or *E. c*^{MC4100}, GanhM4 was predominantly detected in its hydrolyzed form within guts and fat body tissues, with organs from *E. cc*¹⁵ infected flies showing higher levels of the peptide stem compared to *E. c*^{MC4100} fed flies (Fig. 2a, b and Fig. S1d, e). As expected, in *PGRP-LB* mutant flies, the ratio of transformed to untransformed GanhM4 was higher than in wild-type flies (Fig. 2a, b). In clear contrast, gut-derived GanhM4 was predominantly detected in its immunogenic form within the hemolymph of both wild type and *PGRP-LB*^Δ flies infected with *E. cc*¹⁵ or *E. c*^{MC4100} (Fig. 2c). Together, our results suggest that in the early stages of infection, immunogenic PGN fragments rapidly disseminate from the gut lumen to the hemolymph while being internalized and hydrolyzed in surrounding organs. In addition, these findings provide compelling evidence that active ligands of the IMD/NF-κB pathway have the ability to infiltrate tissues in proportion to the quantity released by the bacterial strain present in the gut. Consistently, there was a marked elevation in the intensity of IMD/NF-κB activation, as measured by the expression levels of the target antimicrobial peptide gene *Diptericin-B* (*DptB*), observed in enterocytes and fat body cells of flies infected with *E. cc*¹⁵ in comparison to those infected with *E. c*^{MC4100} (Fig. S2a, b). This pattern was evident in both wild-type and *PGRP-LB* mutant flies (Fig. S2a, b). Overall, these results show that gut-derived GanhM4 from either *E. cc*¹⁵ or *E. c*^{MC4100} elicits a local and systemic activation of the IMD pathway. In addition, they suggest that the high immunogenicity of *E. cc*¹⁵ is directly linked to its ability to release larger quantities of muropeptides, especially GanhM4, able to cross the intestinal epithelium and come into contact with organs and tissues bathed in hemolymph.

2.3. GanhM4 is detected within the brains of *E. cc*¹⁵ fed flies where it activates NF-κB signaling

Given the fact that the nervous system of flies floats in the hemolymph (Limmer et al., 2014), and that previous genetic evidence suggests that PGN-derived muropeptides have the potential to influence fly behavior by interacting with neurons (Kurz et al., 2017; Masuzzo et al., 2019), our investigation focused on detecting the presence of GanhM4 and AEmDapA in the brain's direct environment and in isolated brains of flies orally infected with either *E. cc*¹⁵ or *E. c*^{MC4100}. Utilizing LC-MS, we effectively detected the presence of GanhM4 within intact heads (Fig. 3a), as well as in the tissues surrounding the brain (mainly comprising the trachea and fat body attached to the head capsule) (Fig. 3b), and isolated brains of *E. cc*¹⁵-fed flies while no detection was observed within the brains of *E. c*^{MC4100}-infected flies (Fig. 3c and data not shown). These findings demonstrate that gut-derived GanhM4, present in the hemolymph, has the capacity to interact with brain surface, and enter cells, potentially triggering activation of the IMD/NF-κB pathway. Therefore, we investigated the immunogenicity of gut-born GanhM4 on the brain tissue by analyzing the transcription of *DptB* at 4 and 16 h post-oral infection with *E. cc*¹⁵ and *E. c*^{MC4100}. Our results revealed that the presence of *E. cc*¹⁵ in the intestinal tract rapidly provokes the expression of *DptB* in the brain, with this expression continuing to increase over time (Fig. 3d). Although the level of expression was noticeably lower compared to the one observed after *E. cc*¹⁵ infection, *E. c*^{MC4100} oral infection also triggered a swift induction of *DptB* (Fig. 3d). As anticipated, in the absence of *PGRP-LB* to modulate the biological activity of GanhM4, the transcription of *DptB* was strongly enhanced following both *E. cc*¹⁵ and *E. c*^{MC4100} infections (Fig. 3d). These results provide evidence that gut-derived GanhM4 induces a systemic,

dose-dependent expression of an antimicrobial peptide (AMP) controlled by the IMD/NF-κB pathway in the brain. The capacity of GanhM4 to directly induce cell-autonomous expression of *DptB* in the CNS was corroborated through *ex vivo* incubation experiments. Both purified PGN and GanhM4 were capable of dose-dependently activating *DptB* transcription in isolated brains (Fig. 3e). Taken together, these findings suggest a model in which muropeptides derived from enteric bacteria, notably GanhM4, exit the gut, reach the brain microenvironment, and subsequently regulate gene expression in the brain.

2.4. Oral infection with *E. cc*¹⁵ modulates the brain transcriptome in a GanhM4 dose dependent manner

To obtain a comprehensive and detailed understanding of the genes whose expression is modulated in the brain in response enteric infection, we conducted a transcriptomic analysis using RNA sequencing. This gene expression profiling was conducted 16 h after oral infection in both wild-type and *PGRP-LB*^Δ flies to determine the contribution of GanhM4 to transcriptional regulation of genes. We chose *E. cc*¹⁵ to perform oral infection as our findings demonstrate that GanhM4 derived from this bacteria can be detected within the brain and robustly induces *DptB* expression compared to *E. c*^{MC4100}. Using ± 1.5-fold and a *p*-value 0.05 as cut-off parameters, we identified 245 transcripts showing increased expression following infection (Fig. 4a and Supplemental Data 1) and 63 transcripts showing reduced expression in the wild-type genetic background (Fig. S3a and Supplemental Data 2). Subsequently, we carried out Gene Ontology (GO) and Kyoto Encyclopedia of Genes and Genomes (KEGG) analyses on the upregulated transcripts to identify functional classes of genes whose expression is induced upon infection. The exploration of the GO terms primarily revealed genes linked with immune functions such as “innate immune response” and “response to bacterium” while KEGG pathway analyses showed an enrichment in Toll and IMD signaling (Fig. 4c and e). In contrast, GO term and KEGG pathway analyses of the downregulated genes showed no specific enrichment of any particular biological functions or pathways (Fig. S3b). Using identical cut-off parameters, we observed a substantial upregulation of 1370 genes following infection (Fig. 4b and Supplemental Data 3), along with the downregulation of 439 genes in *PGRP-LB*^Δ flies fed with *E. cc*¹⁵ (Fig. S3c and Supplemental Data 4). The GO terms associated with these genes showed a strong enrichment of immune response-related genes, similar to what was observed in the wild-type genetic background (Fig. 4d). Additionally, KEGG pathway analyses revealed a notable enrichment of the Toll and IMD pathways, along with metabolic pathways, in the mutant context (Fig. 4f). Conversely, as with infected wild-type flies, GO term and KEGG pathway analyses of down-regulated genes in *PGRP-LB* mutant flies did not reveal significant enrichment of specific biological functions or pathways (Fig. S3d, e).

Remarkably, a subset of 147 genes commonly upregulated in both wild-type and *PGRP-LB* mutant can be divided into two distinct clusters (Fig. 4g-h). Cluster 1 includes genes whose expression is amplified further in *PGRP-LB*^Δ, demonstrating that increased GanhM4 levels not only broaden the number of upregulated genes but also boost the expression of genes that are already upregulated in the wild-type context. Cluster 2 consists of genes that exhibit comparable upregulation levels in both scenarios, suggesting these genes may operate independently of GanhM4 levels. Further examination of the GO terms associated with Cluster 1 genes and the enriched pathways within this

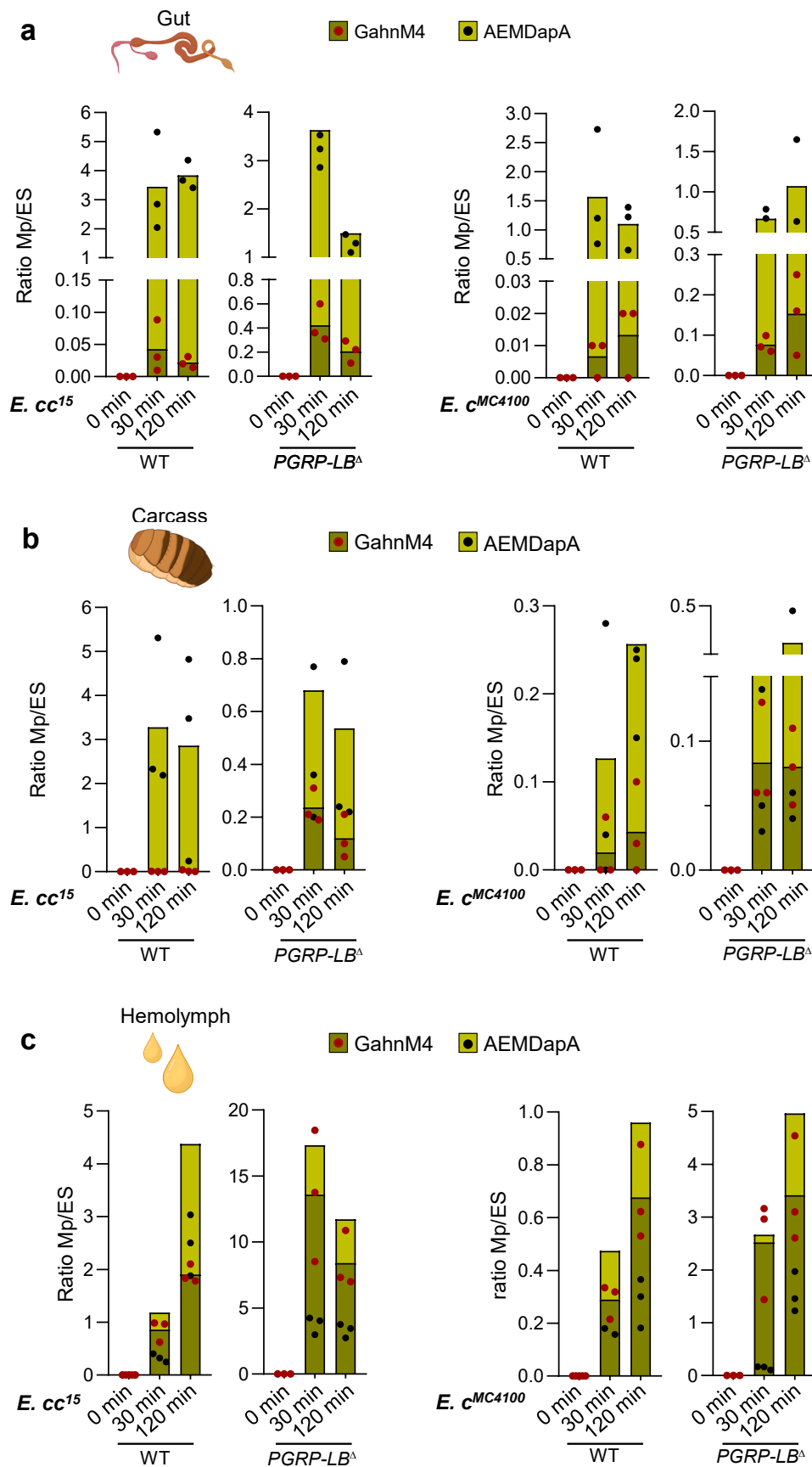
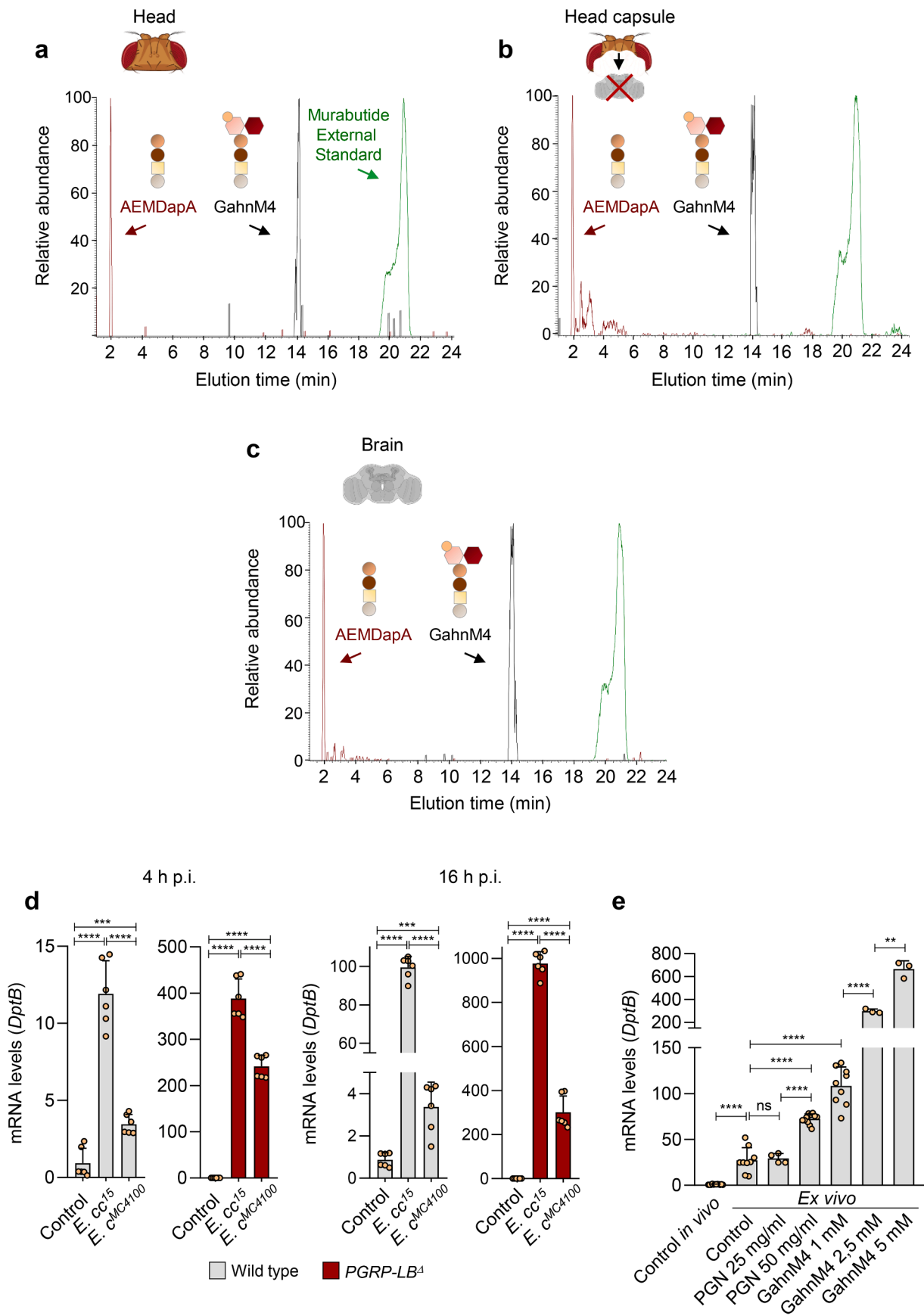


Fig. 2. Tissue-specific quantification of GanhM4 and AEmDapA in *E. cc15* and *E. c^{MC4100}* orally infected flies. (a-c) LC-MS quantification of GanhM4 and the peptide stem AEmDapA in dissected guts (a), carcasses (b), and hemolymph (c) of wild-type and *PGRP-LB* mutant flies under control conditions, 30 min, and 120 min post-oral infection with *E. cc15* or *E. c^{MC4100}*. Each sample (n = 3) consisted of 20 dissected guts or carcasses, and hemolymph was extracted from 60 flies.



(caption on next page)

Fig. 3. Detection of GanhM4 and its peptide stem derivative in brains of orally infected flies and activation of the IMD/NF- κ B pathway. (a–c) Representative LC-MS analysis of GanhM4 and the peptide stem AEmDapA, including the NOD2 agonist murabutide as an external standard, in heads (a), tissues surrounding the brain (trachea and fat body attached to the head cuticle) (b), and isolated brains (c) of wild-type flies at 120 min post-oral infection with *E. cc*¹⁵. Each sample consisted of 20 dissected heads, head capsules, or brains. (d) Quantitative RT-PCR analysis of the expression of the IMD/NF- κ B target gene *DptB* in dissected brains of wild-type and *PGRP-LB* mutant flies under control conditions and at 4 and 16 h post-oral infection with *E. cc*¹⁵ or *E. cc*^{MC4100}. (e) Quantitative RT-PCR analysis of the expression of *DptB* in dissected brains of wild-type flies after 16 h of *ex-vivo* culture with increasing concentrations of *E. c* purified PGN or highly purified *E. cc*¹⁵ GanhM4. Comparisons between selected conditions in (d) and (e) are shown (unpaired *t*-test, ns = not significant, *****p* < 0.0001, ****p* < 0.001, ***p* < 0.01, and **p* < 0.1).

cluster affirms the predominance of immune response-related genes and the Toll and IMD pathways (Fig. 4i–j). In contrast, for Cluster 2 genes, the associated GO terms are limited to the abiotic process “response to cold” and “response to bacterium” (Fig. 4k). Overall, our transcriptomic analyses indicate that oral infection with *E. cc*¹⁵ mediated GanhM4 dose-dependent changes in the physiology of the brain with essentially an increase of defense and immune functions.

2.5. Gut derived GanhM4 triggers immune and stress signaling pathways in the brain

To gain deeper insights into the regulatory networks governing the brain’s response to oral infection with *E. cc*¹⁵, we examined the transcriptional upregulation of signaling components identified in the RNAseq analysis. As expected, given the Gram-negative nature of the *E. cc*¹⁵ bacterium, there was a substantial enrichment of the IMD/NF- κ B associated target genes among the most strongly induced genes highlighting a key role of this signaling pathway in regulating the brain immune response (Fig. 5). These genes include numerous effectors such as AMP genes (notably the *Diptericin*, *Cecropin*, and *Attacin* genes) (Fig. 5 and Fig. S4a), which directly inhibit pathogen proliferation, and *PGRP* encoding genes, which have the ability to bind to peptidoglycan fragments and its derivative GanhM4 (Myllymäki et al., 2014) (Fig. 5 and Fig. S4b). The binding activity of the *PGRPs* identified in our analysis can either facilitate PGN degradation (*PGRP-LB*, *PGRP-SC1b/2*, *PGRP-SB1/2* (Paredes et al., 2011)) or prevent the spontaneous activation of the IMD pathway (*PGRP-LF* (Maillet et al., 2008)) thereby curtailing the immune response, or eventually trigger IMD pathway activation (*PGRP-LC* (Gottar et al., 2002) and *PGRP-SD* (Iatsenko et al., 2016)), augmenting the immune defense (Fig. 5 and Fig. S4b, c). The significant presence of these *PGRP*-related genes, some of which are predicted orthologs of the *PGLYRP* mammalian peptidoglycan sensing genes (Fig. 5), underscores the importance of PGN recognition and processing in the brain’s response to gut-associated *E. cc*¹⁵ infection. Furthermore, the NF- κ B transcription factor *relish* (*rel*) (Dushay et al., 1996), a key positive regulator of the IMD pathway effectors as well as *pirk* (Kleino et al., 2008), a cytoplasmic negative regulator that modulates IMD pathway activity to the severity of infection, were also found to be upregulated (Fig. 5 and Fig. S4c). Remarkably, the transcription of all AMP and *PGRP* genes was significantly enhanced in the *PGRP-LB* mutant, providing further evidence of a GanhM4 dose-dependent regulation of IMD/NF- κ B-associated genes (Fig. 5 and Fig. S4a–c).

We also observed the moderate induction of several Toll pathway-related genes in our dataset, particularly in *PGRP-LB* mutants (Fig. 5). This includes *spätzle* (*spz*) (Lemaitre et al., 1996), a ligand for Toll, *PGRP-SA* (Michel et al., 2001), a gene encoding a secreted protein that mediates Toll pathway activation during bacterial infection, and target genes encoding secreted immune-induced peptides such as *GNBP1*, *Drsl1*, *Drsl6*, *IM4*, *IM14*, and most members of the *Bomanin* gene family (*BomS1-5*, *BomBc1-3* and *BomT1-3*) (Clemmons et al., 2015) (Fig. 5). In *Drosophila*, the Toll pathway is conventionally associated with defense against Gram-positive bacteria and fungi (Michel et al., 2001). While the abundance of Toll pathway genes is intriguing, considering that *E. cc*¹⁵ is a Gram-negative bacterium, these results confirm previous observations showing that Gram-negative peptidoglycans are able to activate the Toll pathway in certain contexts (Leulier et al., 2003). The presence of Toll pathway genes in the *PGRP-LB* mutant, where GanhM4 levels are elevated, raises the possibility that an overabundance of GanhM4 could

trigger a broad-based immune response activating multiple defense pathways, including Toll and IMD pathways.

In addition, a number of genes encoding components of the Janus kinase (JAK)-signal transducer and activator of transcription (STAT) pathway, which is considered a key pathway regulating the immune response along with IMD/NF- κ B and Toll signaling (Myllymäki and Rämetsä, 2014), were also found to be induced in wild type dissected brains (Fig. 5). This notably includes two of its ligands: *unpaired-2* (*upd-2*), a structural and functional ortholog of the primary human adipokine *LEPTIN*, and *unpaired-3* (*upd3*), as well as the fly *GATA4* ortholog *pannier* (*pnr*), and three members of the *Turandot* gene family encoding stress-induced humoral factors (*TotA*, *TotC*, and *TotM*) (Agaisse et al., 2003) (Fig. 5 and Fig. S4d). With the exception of *pnr* and *TotC*, all additional signaling components associated with the JAK/STAT pathway showed an enhancement in expression in the *PGRP-LB* mutant (Fig. 5). These results suggest that, in addition to the IMD/NF- κ B and Toll pathways, the presence of *E. cc*¹⁵ in the intestinal tract results in a GanhM4-dose dependent activation of the evolutionary conserved JAK/STAT signaling pathway in the brain.

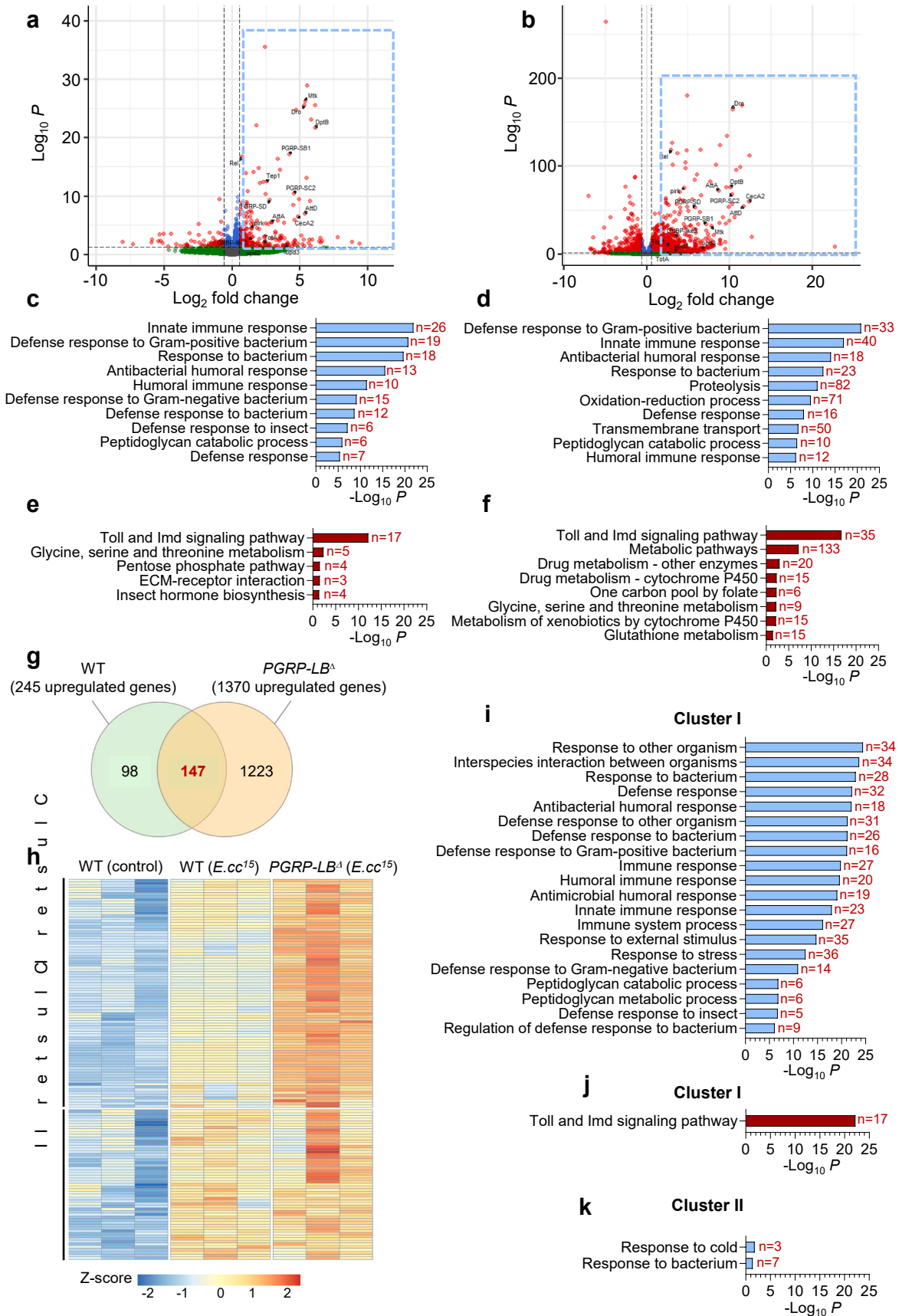
To validate the RNA seq data analysis, we examined the expression of a representative subset of *E. cc*¹⁵-induced genes in both wild-type and *PGRP-LB*^Δ brains using RT-qPCR. The gene selection included ten AMP genes (*Attacin-A*, *-B*, and *-C*, *Cecropin-A1*, *-A2*, and *-C*, *CG45045*, *Dipt-B*, *GNBP-like3*, and *Metchnikowin*), six *PGRP* genes (*PGRP-LB*, *-SB1*, *-SC2*, *-SD*, *-LF*, and *-SA*), and three *Turandot* genes (*TotA*, *TotC*, and *TotM*) (Fig. 6). Additionally, to extend our analysis and assess the contribution of the IMD pathway, we measured the transcript levels of the selected genes in *E. cc*¹⁵-fed flies carrying a loss-of-function mutation of *Fadd* (*Fadd*^Δ), an adapter protein functioning downstream of IMD (Leulier et al., 2002) (Fig. 6a–c). Our results confirmed that all AMP and *PGRP* genes tested, including the Toll activator *PGRP-SA*, were transcriptionally up-regulated upon intestinal infection (Fig. 6a, b). Moreover, this induction was enhanced in *PGRP-LB* mutants and greatly reduced in *Fadd* mutants (Fig. 6a, b). In contrast, the transcription of *TotA*, *TotC*, and *TotM* was clearly enhanced in *PGRP-LB*^Δ but not inhibited in *Fadd*^Δ flies, suggesting that GanhM4 modulates the level of transcription of JAK/STAT associated genes in an IMD-independent manner (Fig. 6c).

To definitively establish whether the higher gene inducibility observed in *PGRP-LB*^Δ flies was directly dependent on circulating GanhM4 levels, we further compared the transcript levels of our gene selection in wild-type controls and in flies in which the secreted form of *PGRP-LB* (*PGRP-LB*^{RC} (Charroux et al., 2018)) was ectopically expressed in the fat body and consequently in the surrounding hemolymph. Our results established that, with the exception of *AttA* and *PGRP-SB1*, the increased level of *PGRP-LB*^{RC} was associated with reduced inducibility of all selected AMP, *PGRP*, and *Turandot* genes (Fig. 6d–f).

Collectively, the view of gene expression profiling reveals that oral ingestion of *E. cc*¹⁵ primarily triggers the IMD/NF- κ B signaling pathway, while also leading to activation of the Toll and JAK/STAT immune pathways. Furthermore, it identifies gut-derived GanhM4 as a critical modulator of the brain’s innate immune response.

2.6. GanhM4 drives gene expression of IMD/NF- κ B target genes in glial cells and neurons

The primary activation of the IMD/NF- κ B signaling pathway in the CNS upon ingestion of *E. cc*¹⁵ suggests that brain cells can detect and



(caption on next page)

Fig. 4. Comparative transcriptomic analysis of fly brain response to oral infection with *E.cc*¹⁵. **(a–b)** Volcano plots illustrating the proportion of differentially expressed genes in isolated brains of wild-type (a) and *PGRP-LB* mutant flies (b) at 16 h post-oral infection with *E.cc*¹⁵. Genes within the blue squares were selected based on a + 1.5-fold change and a p-value of 0.05 as cut-off parameters. **(c–f)** Functional analysis using DAVID GO terms (blue bar plots) and KEGG pathway enrichment (red bar plots) for up-regulated genes in dissected brains of infected wild-type (c and e) and *PGRP-LB* mutant flies (d and f). **(g)** Venn diagram displaying genes commonly up-regulated in the brains of wild-type and *PGRP-LB* mutant flies orally exposed to *E.cc*¹⁵. **(h)** Clustering heatmap demonstrating the classification of genes commonly up-regulated in the brains of infected wild-type and *PGRP-LB* mutant flies. **(i–k)** Functional analysis utilizing DAVID GO terms (i, k) and KEGG pathway enrichment (j) for genes in clusters I and II (h). KEGG pathway analysis for genes in cluster II did not reveal significant enrichment of specific biological functions or pathways. (For interpretation of the references to colour in this figure legend, the reader is referred to the web version of this article.)

respond to gut-derived GanhM4. Like mammals, the fly brain consists primarily of glial cells and neurons. To identify in which cell subtype the NF- κ B signaling is activated in response to circulating GanhM4, we initially examined the inducibility of ten AMPs after inhibiting IMD pathway activation via RNAi-mediated silencing of *Fadd* in either glial cells or neurons. A significant decrease in the transcription of all AMPs occurred upon blocking IMD pathway activation in glial cells; however, RNAi-mediated knockdown of *Fadd* in neurons also affected the expression of several AMPs, including *AttD* and *Mtk*, albeit to a lesser extent (Fig. 7a). To further assess the competence of glial cells and neurons to trigger AMPs expression in response to IMD activation, AMP expression levels were analyzed after constitutively activating IMD/NF- κ B signaling by overexpressing IMD in each cell type (Georgel et al., 2001). Remarkably, only the activation of the IMD cascade in glial cells induced the expression of AMPs, not in neurons (Figure S5). These results suggest that during infection, while the activation of the IMD pathway in neurons might impact the expression of antimicrobial peptides, this primarily relies on the activation of the IMD cascade in glial cells. The inducibility of six *PGRP* genes after silencing *Fadd* in glial cells and neurons was also analyzed. A clear decrease in the transcription of *PGRP-LF*, *-SA*, *-SB1*, and *-SC2* was observed when inactivating the IMD/NF- κ B pathway in glial cells (Fig. 7b). Exceptions include *PGRP-SD*, whose expression is significantly inhibited after *Fadd* silencing in glial cells, but to a lesser extent when IMD activation is blocked in neurons; and *PGRP-LB*, which shows clear inhibition after silencing *Fadd* in neurons but not in glial cells (Fig. 7b). Altogether, these results support the notion that gut-derived GanhM4 can stimulate gene expression in the CNS by activating the IMD/NF- κ B signaling pathway in both glial cells and neurons.

In the adult *Drosophila* brain, glial cells can be classified into five cell types that perform functions similar to those of astrocytes, oligodendrocytes, and microglial cells, the principal glial subtypes in the mammalian CNS (Yildirim et al., 2019) (Table 1). The perineurial and subperineurial glial cells are located at the outer surface of the nervous system, forming the outer and inner layers of the blood-brain barrier (BBB), which separates the nervous system from the hemolymph (Stork et al., 2008). On the other hand, astrocyte-like, ensheathing, and cortex glia are found within the central nervous system, contributing to neural development and functioning (Kremer et al., 2017). To gain insights into the glial cell type(s) dependent on functional NF- κ B for gene transcription in response to *E.cc*¹⁵ oral infection, we selectively silenced *Fadd* via RNAi in each glial cell subtype and assessed the expression of *DptB* using qRT-PCR. Our results showed that the up-regulation of *DptB* was significantly inhibited only when the IMD pathway was inactivated in perineurial cells (Fig. 7c). To explore whether this result applied to more IMD/NF- κ B targets, we further analyzed the expression of nine additional AMP and six *PGRP* genes. We observed a significant reduction in the transcription of all AMP genes as well as *PGRP-SB1*, *-SC2*, and *-SD* after knocking down *Fadd* in perineurial cells (Fig. 7d, e). However, reducing immune signaling in perineurial cells did not affect the expression of *PGRP-LF* or *PGRP-SA*, suggesting that these genes are controlled through the activation of the IMD/NF- κ B pathway in another glial cell subtype (Fig. 7e). Furthermore, in line with our previous findings demonstrating the dependence of IMD/NF- κ B activation in neurons (Kurz et al., 2017; Masuzzo et al., 2019), the induction of *PGRP-LB* was also not affected following *Fadd* silencing in perineurial cells (Fig. 7e). Our comprehensive results demonstrate that in the brain,

sensing of gut-derived GanhM4 leads to the activation of IMD/NF- κ B signaling pathways in both neurons and different glial cell subtypes, thereby inducing the expression of distinct immune effectors. In particular, the production of AMP peptide genes, a key aspect of host defense, appears to rely on the activation of the IMD/NF- κ B signaling pathway in perineurial glial cells. To further ascertain the identity of cells responsible for AMP expression in the brain in response to gut-derived GanhM4, we analyzed the expression profile of different AMP-GFP reporter transgenes. Remarkably, *E.cc*¹⁵ oral infection exclusively increased *DptB* expression in the outermost cell layer of the central nervous system, overlapping with perineurial cell markers (Fig. 8, Figure S6 and Figure S7). Similar results were obtained using *Attacin-A-GFP* and *Metchnikowin-GFP* reporters (Figure S7 and figure S8), conclusively identifying these cells as the primary contributors to AMP production in the brain upon detection of circulating GanhM4. Altogether our findings support a direct dialogue between enteric bacteria and the brain in *Drosophila* and establish GanhM4 as a pivotal modulator of brain immunity through glial and neuronal NF- κ B signaling cascades.

2.7. Chronic IMD/NF- κ B signaling in perineurial glia is associated with neurological decline

Genetic mutations resulting in the constitutive activation of the IMD/NF- κ B pathway in the CNS shorten flies' lifespan and correlate with neurological decline, as evidenced by early locomotor defects and neurodegeneration (Kounatidis et al., 2017). Given that persistent colonization of the gastrointestinal tract with *E.cc*¹⁵ induces sustained PGN-dependent systemic activation of the IMD/NF- κ B pathway and premature death (Zugasti et al., 2020), we investigated whether enteric infection could remotely trigger phenotypes associated with neurological decline. To assess locomotor capacities, we conducted climbing assays, utilizing the natural tendency of flies to move against gravity when agitated, a behavior known as negative geotaxis (Ali et al., 2011). Additionally, we employed a histological approach to quantify neuronal degeneration by measuring the number of vacuoles appearing in the fly brain upon chronic oral infection. Our results demonstrate that both chronically infected wild type and *PGRP-LB*^Δ flies displayed an early age reduction in locomotor activity compared to non-infected flies, with a locomotion-based behavior decline exacerbated in *PGRP-LB* mutants (Fig. 9a). Remarkably, this infection-dependent reduction in climbing performance was completely suppressed in flies carrying a null mutation in the *caspace-8* homolog *Dredd*, a component of the IMD pathway required for innate immune signaling (Meinander et al., 2012). Alongside locomotor defects, the brains of wild type *E.cc*¹⁵-infected flies exhibited more vacuoles compared to those of uninfected flies, a phenotype exacerbated in *PGRP-LB* mutants and fully rescued in *Dredd*-null flies (Fig. 9c, d). Together, these results confirm that chronic *E.cc*¹⁵ enteric infection is accompanied by neurological decline dependent on the amount of circulating GanhM4 and the intensity of activation of the IMD/NF- κ B pathway.

Besides activating immune signaling in enterocytes and fat body cells, we found that, in the brain, *E.cc*¹⁵-derived GanhM4 also triggers immune signaling in perineurial glial cells. Consequently, we explored whether inducing the IMD/NF- κ B cascade in these brain cells resulted in phenotypes associated with neurological decline. Our findings demonstrate that constant immune signaling in perineurial glia via IMD overexpression significantly reduced fly lifespan and age-dependent

Gene name	Wild type		<i>PGRP-LB</i> ¹		Gene description/function	Pathway(s)	Predicted ortholog(s)	
	Fold change	p-value	Fold change	p-value			Human	Mouse
<i>DptB</i> *	70,68	1,91E-22	1116,69	1,10E-76	Antimicrobial peptide	IMD		
<i>DptA</i>	69,58	2,74E-26	2930,81	4,11E-170	"	IMD		
<i>CecA1</i> *	56,45	7,35E-24	2545,29	1,35E-99	"	IMD		
<i>CecB</i>	53,34	6,57E-10	1578,45	1,14E-42	"	IMD		
<i>CecC</i> *	46,27	1,26E-29	460,92	1,05E-124	"	IMD		
<i>AttC</i> *	44,71	6,76E-14	853,76	3,80E-135	"	IMD		
<i>Mtk</i> *	42,30	5,50E-27	223,38	9,54E-33	"	IMD		
<i>AttD</i> *	40,98	1,05E-07	3305,26	5,10E-55	"	IMD		
<i>Dro</i>	39,87	2,42E-26	1352,58	1,73E-165	"	IMD		
<i>Def</i>	30,53	3,78E-10	782,78	1,15E-76	"	IMD/Toll		
<i>CecA2</i> *	28,64	2,84E-07	5226,37	3,98E-60	"	IMD		
<i>CG45045</i> *	26,15	1,47E-25	1257,21	7,97E-58	"	IMD		
<i>AttB</i> *	23,92	1,21E-06	957,01	1,26E-54	"	IMD		
<i>Listericin</i>	14,27	4,27E-06	171,98	7,79E-24	"	IMD/JAK-STAT		
<i>CG43236</i>	10,19	3,78E-17	75,39	7,75E-17	"	IMD		
<i>Drs</i>	7,65	3,10E-06	62,99	1,08E-28	"	IMD/Toll		
<i>AttA</i> *	7,56	2,81E-06	424,63	1,04E-72	"	IMD/Toll		
<i>GNBP-like3</i>	2,75	1,00E-03	11,18	1,26E-20	"	IMD		
<i>GNBP1</i>	0,90	4,02E-01	1,79	1,32E-04	"	Toll		
<i>Drsl1</i>	NA	NA	102,18	2,38E-05	"	Toll		
<i>Drsl6</i>	NA	NA	281,46	7,57E-10	"	Toll		
<i>Cec2</i>	NA	NA	44,74	3,22E-03	"	IMD/Toll		
<i>Cec-Psi1</i>	NA	NA	149,15	7,42E-07	"	/		
<i>BomS1</i>	1,62	9,53E-03	12,84	1,60E-57	AMP-like	Toll		
<i>BomS2</i>	1,26	1,56E-01	4,33	2,61E-05	"	Toll		
<i>BomS3</i>	1,29	2,81E-02	5,92	9,87E-33	"	Toll		
<i>BomS4</i>	1,77	1,29E-02	4,21	3,44E-08	"	Toll		
<i>BomS5</i>	1,96	4,55E-02	5,93	7,04E-20	"	Toll		
<i>BomBc1</i>	1,78	2,16E-01	24,01	1,65E-15	"	Toll		
<i>BomBc2</i>	1,11	7,56E-01	3,14	2,25E-03	"	Toll		
<i>BomBc3</i>	1,66	1,10E-03	2,93	2,32E-04	"	Toll		
<i>BomT1</i>	1,50	1,99E-01	13,57	4,26E-22	"	Toll		
<i>BomT2</i>	1,25	3,02E-01	3,03	1,50E-03	"	Toll		
<i>BomT3</i>	1,27	4,04E-01	2,93	1,24E-02	"	Toll		
<i>edin</i>	4,03	1,34E-02	5597,37	5,43E-113	Secreted peptide	IMD		
<i>IM4</i>	1,38	1,48E-01	2,33	4,13E-02	"	Toll		
<i>IM14</i>	1,43	8,16E-02	2,94	2,97E-02	"	Toll		
<i>IM33</i>	2,14	3,52E-07	10,57	3,08E-09	"	/	<i>EPPIN</i>	<i>Eppin</i>
<i>Hayan</i>	2,18	1,54E-03	15,05	3,82E-14	"	Toll	<i>PRSS33, PROC, F12</i>	<i>C1rl, Gzmg, Gzmf</i>
<i>PGRP-SC1b</i>	7,75	2,36E-01	240,31	4,62E-10	Amidase	IMD	<i>PGLYRP1</i>	<i>Pglyrp1</i>
<i>PGRP-SC2</i> *	23,41	3,56E-11	1305,32	6,57E-69	"	IMD	<i>PGLYRP1</i>	<i>Pglyrp1</i>
<i>PGRP-SB1</i> *	18,57	6,17E-18	148,14	1,05E-34	"	IMD	<i>PGLYRP2</i>	<i>Pglyrp4, Pglyrp1</i>
<i>PGRP-SB2</i>	15,78	1,71E-01	24,01	3,16E-02	"	IMD	<i>PGLYRP1/2</i>	<i>Pglyrp1</i>
<i>PGRP-LB</i> *	1,85	8,88E-05	6,35	1,00E-22	"	IMD	<i>PGLYRP2</i>	<i>Pglyrp2</i>
<i>PGRP-SD</i> *	6,85	4,31E-10	58,66	1,00E-53	Pathogen recognition	IMD	<i>PGLYRP1</i>	<i>Pglyrp1</i>
<i>PGRP-LF</i> *	4,89	3,41E-13	29,83	4,44E-54	"	IMD	<i>PGLYRP1/3/4</i>	<i>Pglyrp1</i>
<i>PGRP-SA</i> *	2,67	5,94E-06	16,21	1,40E-71	"	Toll	<i>PGLYRP1</i>	<i>Pglyrp1</i>
<i>PGRP-LC</i>	1,01	9,20E-01	5,98	2,78E-11	"	IMD	<i>PGLYRP1/4</i>	<i>Pglyrp1</i>
<i>Tep1</i>	5,83	3,24E-13	6,57	1,79E-10	"	IMD/Toll	<i>CD109</i>	<i>CD109</i>
<i>Tep2</i>	1,37	2,59E-01	3,75	2,38E-22	"	Toll	<i>CD109</i>	<i>CD109</i>
<i>Tep3</i>	0,72	9,85E-01	1,89	6,36E-05	"	Toll	<i>CD109</i>	<i>CD109</i>
<i>Tep4</i>	1,19	9,99E-01	25,42	1,49E-98	"	Toll	<i>CD109</i>	<i>CD109</i>
<i>lectin-24A</i>	0,90	9,01E-01	4,69	1,38E-02	"	/	<i>MBL2, SFTPD, COLEC10</i>	<i>Cd207, clec4f, Cd209g/e colec10</i>
<i>NimB1</i>	1,22	1,33E-01	2,85	5,30E-04	"	/	<i>MEGF10/11</i>	<i>Megf10</i>
<i>NimB2</i>	1,60	5,92E-04	2,88	2,46E-04	"	/	<i>MEGF10/11</i>	<i>Megf10</i>
<i>NimB3</i>	1,80	1,80E-02	2,79	1,02E-04	"	/	<i>PEAR1</i>	<i>Pear1</i>
<i>NimB5</i>	1,66	1,07E-03	1,70	3,47E-03	"	/	<i>STAB1/2, MGEF10/11, PEAR1</i>	<i>Megf10/11, Pear1, Scarf2</i>
<i>pirk</i>	2,78	3,82E-05	23,15	7,09E-76	IMD pathway regulator	IMD		
<i>rel</i>	1,67	1,62E-17	7,87	1,87E-119	Transcription factor	IMD	<i>NFKB1/2</i>	<i>Nfkb2</i>
<i>pnr</i>	2,03	4,06E-05	1,58	3,02E-02	"	JAK-STAT	<i>GATA4</i>	<i>Gata4</i>
<i>TotA</i> *	5,11	1,10E-02	7,01	1,45E-02	Stress peptide	JAK-STAT		
<i>TotM</i> *	9,23	1,09E-04	41,13	1,40E-05	"	JAK-STAT		
<i>TotC</i> *	6,51	1,25E-02	5,31	3,94E-02	"	JAK-STAT		
<i>Sid</i>	0,99	9,85E-01	6,15	1,59E-11	Enzyme	Toll	<i>EXOG</i>	<i>Exog</i>
<i>CG8046</i>	1,67	8,85E-04	2,95	7,99E-07	Petidoglycan transporter	/	<i>SLC46A3/A1</i>	<i>Slc46a1</i>
<i>upd2</i>	4,34	4,53E-02	10,41	6,72E-04	Cytokine	JAK-STAT	<i>LEP</i>	
<i>upd3</i>	15,44	2,42E-02	102,74	6,65E-07	"	JAK-STAT		
<i>Diedel</i>	3,53	4,14E-02	8,06	2,74E-02	"	IMD		
<i>Tollo</i>	0,96	7,00E-01	1,91	4,12E-08	Toll-like receptor family	Toll	<i>TLR3/4/7</i>	<i>Tlr-3/4/13</i>
<i>spz</i>	1,06	5,03E-01	2,68	8,86E-16	Secreted peptide	Toll		

Fold change : <1,5 > 1,5 > 5 > 15 > 80

Fig. 5. Selection of genes up-regulated in the brain following *E. cc*¹⁵ oral infection. Genes are listed with their name, fold change (compared to unchallenged wild-type flies), p-values, functions, and associated pathways in both wild-type and *PGRP-LB* mutant flies. Genes marked with an asterisk (*) had their expression profiles confirmed through quantitative RT-PCR analysis using independent brain samples. The *Drosophila* RNAi Screening Center Integrative Ortholog Prediction Tool (DIOPT) (Hu et al., 2011) was used to determine human and mouse orthologs of fly genes (highest confidence predictions are indicated in bold).

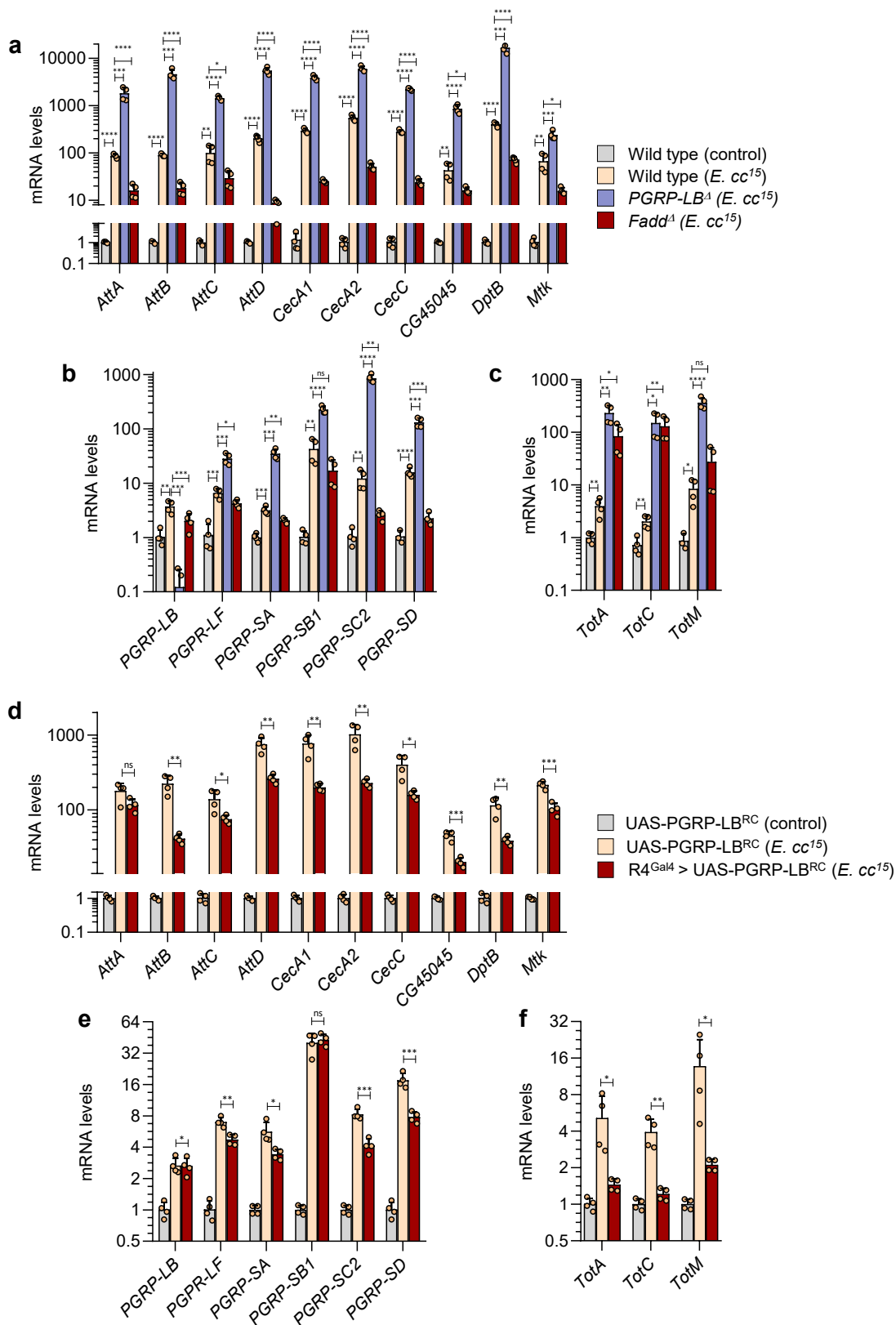


Fig. 6. Contribution of IMD/NF- κ B pathway and gut-derived muuropeptides present in the hemolymph to the expression of selected brain up-regulated genes. (a-c) Quantitative RT-PCR analysis of the expression of a selection of genes encoding AMPs (a), PGRPs (b), and components of the JAK/STAT pathway (c) in dissected brains of unchallenged wild-type flies and wild-type, *PGRP-LB*, and *Fadd* mutant flies at 16 h post-oral infection with *E. coli*. (d-f) Quantitative RT-PCR analysis of the expression of genes encoding AMPs (d), PGRPs (e), and components of the JAK/STAT pathway (f) in dissected brains of control flies (UAS-PGRP-LB^{RC}) or flies expressing the secreted isoform of the amidase *PGRP-LB* in the hemolymph (R4^{Gal4} > UAS-PGRP-LB^{RC}) at 16 h post-oral infection with *E. coli*. Comparisons between selected conditions are shown (unpaired *t*-test, ns = not significant, *****p* < 0.0001, ****p* < 0.001, ***p* < 0.01, and **p* < 0.1).

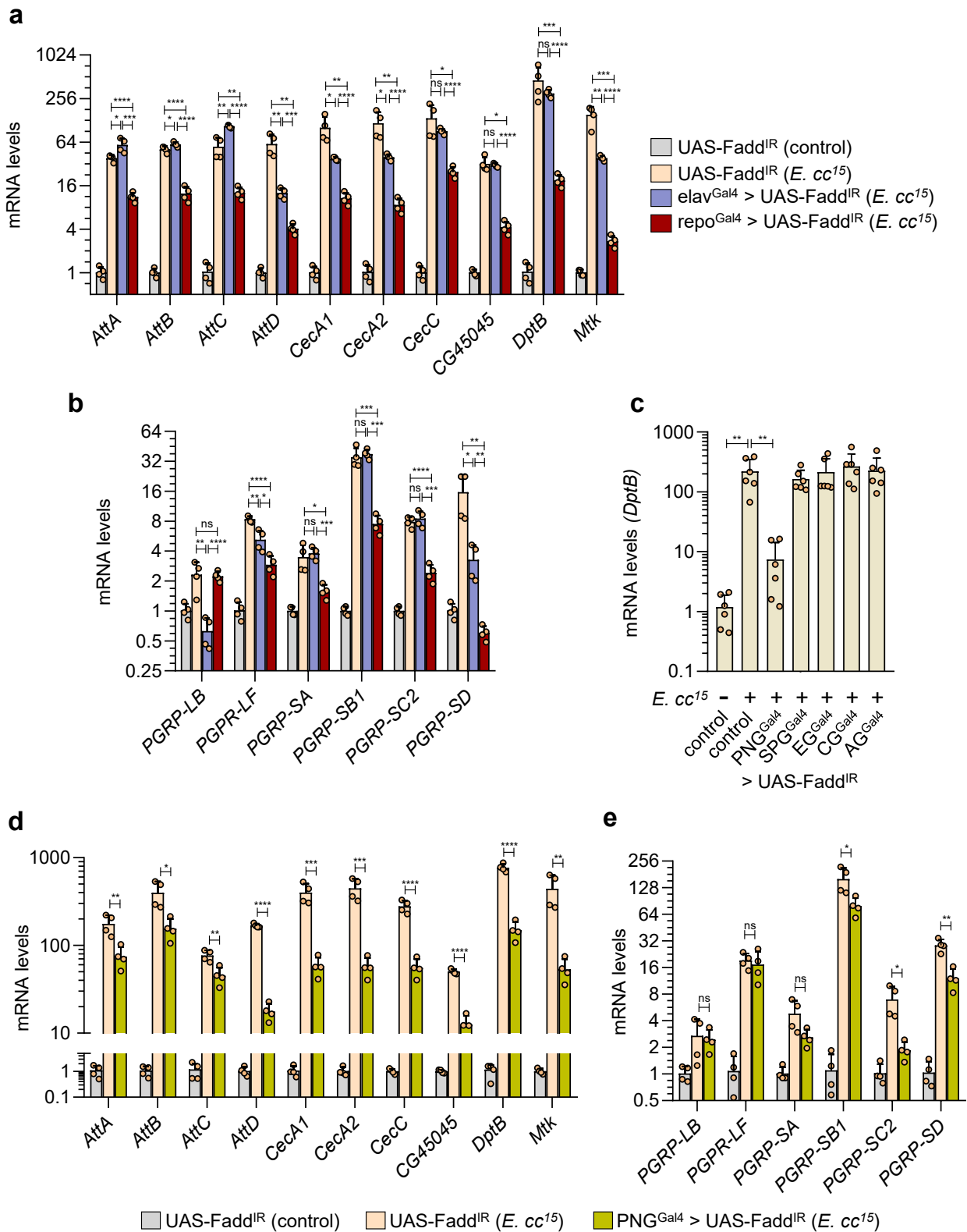


Fig. 7. Contribution of IMD/NF-κB pathway in neural cells to the induction of selected AMP and PGRP encoding genes. (a–b) Quantitative RT-PCR analysis of the expression of genes encoding selected AMPs (a) and PGRPs (b) in dissected brains of control wild-type flies (UAS-Fadd^{IR}) and following RNAi-mediated inactivation of the NF-κB component *Fadd* in neurons (elav^{Gal4} > UAS-Fadd^{IR}) or glial cells (repo^{Gal4} > UAS-Fadd^{IR}) at 16 h post-oral infection with *E. cc*¹⁵. (c) Quantitative RT-PCR analysis of *DptB* expression in brains of control wild-type flies (UAS-Fadd^{IR}) and following *Fadd* RNAi in perineurial glia (PNG^{Gal4} > UAS-Fadd^{IR}), subperineurial glia (SPG^{Gal4} > UAS-Fadd^{IR}), ensheathing glia (EG^{Gal4} > UAS-Fadd^{IR}), cortex glia (CG^{Gal4} > UAS-Fadd^{IR}) and astrocyte-like glia (AG^{Gal4} > UAS-Fadd^{IR}) at 16 h post-oral infection with *E. cc*¹⁵. (d–e) Quantitative RT-PCR analysis of the expression of selected AMPs and PGRPs in brains of control wild-type flies (UAS-Fadd^{IR}) and following *Fadd* RNAi in perineurial glia (PNG^{Gal4} > UAS-Fadd^{IR}) at 16 h post-oral infection with *E. cc*¹⁵. Comparisons between selected conditions are shown (unpaired *t*-test, ns = not significant, *****p* < 0.0001, ****p* < 0.001, ***p* < 0.01, and **p* < 0.1).

Table 1Glial subtypes in the central nervous system: functions and orthologous populations in Mammals and *Drosophila*.

CNS Glia subtypes	Major functions	Mammalian glial cell	<i>Drosophila</i> glial cell
Microglia	<ul style="list-style-type: none"> •Immune defense and response •Surveillance of the CNS microenvironment •Neuroprotection and tissue repair •Modulation of synaptic activity •Regulation of neuroinflammation •Phagocytosis of cellular debris and pathogens 	Microglia	Astrocyte-like, Ensheathing glia, Cortex glia
Astrocytes	<ul style="list-style-type: none"> •Structural support for CNS architecture •Regulation of extracellular environment •Metabolic support for neurons •Neurotransmitter recycling and synthesis •Neuroprotection •Modulation of synaptic function 	Astrocytes	Astrocyte-like
Oligodendrocytes	<ul style="list-style-type: none"> •Myelination of axons •Axonal support and protection •Regulation of ion homeostasis •Neurotransmitter uptake •Synaptic pruning and plasticity 	Oligodendrocytes	Ensheathing glia
Blood Brain Barrier	<ul style="list-style-type: none"> •Regulation of molecular exchange between blood and brain tissue •CNS protection from harmful substances and pathogens •Control of ion, nutrient, and neurotransmitter levels 	Astrocytes	Perineurialglia, Subperineurialglia

climbing ability compared to control flies or those with IMD overexpressed in gut and fat body cells (Fig. 9e, f). Additionally, we found that continuous NF- κ B signaling in perineurial cells resulted in increased vacuolization of the brain compared to control flies (Fig. 9g, h). Collectively, these findings highlight the significance of gut-derived GanhM4 and IMD/NF- κ B signaling in perineurial glia as a major determinant of *Drosophila* lifespan and early neurological decline.

3. Discussion

This comprehensive analysis of the dynamics of PGN fragments dissemination from the intestinal lumen to the systemic circulation, coupled with its transcriptomic impact on the central nervous system, highlights the essential role of monomeric muropeptides as critical mediators of the gut-brain axis. In this context, gut-derived muropeptides function in *Drosophila* in a manner similar to their role in mouse models, transmitting signals from the intestinal tract to the host CNS (Gabanyi et al., 2022; Tosoni et al., 2019; Wheeler et al., 2023).

Our data clearly demonstrate that GanhM4, produced within the gut by two Gram negative bacterial species, undergoes translocation to the hemolymph, where detection occurs within minutes following oral infection. This rapid translocation of GanhM4 from the gut to the hemolymph raises intriguing questions about the mechanisms at play. Several hypotheses, which are not mutually exclusive, might be considered. Firstly, similar to gut bacteria-derived lipopolysaccharide (LPS), another potent stimulator of vertebrates and invertebrates innate immunity derived from the membrane of gram-negative bacteria (Sampath, 2018), monomeric muropeptides could cross the intestinal mucosa by inducing intestinal tight junction permeability in enterocytes or exploiting intercellular gaps between junctions (Guo et al., 2015, 2013). In addition, given that enterocytes possess the capability to internalize peptidoglycan fragments, they could potentially be transported via transcytosis and subsequently released into the hemolymph (Bu et al., 2010; Joshi et al., 2023). Ultimately, it would also be important to explore whether members of the SLC46 family, an evolutionary conserved group of peptidoglycan transporters, contribute actively to the transport of immunogenic muropeptides in this process (Bharadwaj et al., 2023; Paik et al., 2017).

Following translocation from the gut lumen to the hemolymph, our results support the existence of direct sensing of PGN fragments by brain cells. Firstly, LC-MS analysis demonstrated the presence of active muropeptides within brain tissue following oral infection with *E. coli*¹⁵.

Moreover, elevated levels of circulating muropeptides, resulting from the functional inactivation of the peptidoglycan-degrading enzyme *PGRP-LB*, exert a profound impact on the brain's transcriptional response to gut bacterial infection. Furthermore, the functional inactivation of circulating PGN through the ectopic expression of the secreted isoform of *PGRP-LB* leads to a substantial reduction in the transcriptomic impact of intestinal infection on the brain. Finally, direct incubation of the brain with PGN fragments or purified GanhM4 induces a rapid and significant changes in gene expression, further reinforcing the notion of a direct PGN-brain interaction. Although these data support a direct sensing between circulating muropeptides and immune receptors on brain cells, it remains plausible that other immune-responsive cell types, such as *Drosophila* blood cells called hemocytes, which are recruited to the brain following infection, may influence this response (Sanchez Bosch et al., 2019; Winkler et al., 2021). These immune cells have the potential to achieve this by synthesizing proteins that modulate the levels of circulating active PGN (e.g., amidases (Chakrabarti and Visweswariah, 2020; Paredes et al., 2011)) or facilitate the activation of the IMD pathway (e.g., *PGRP-SD* (Chakrabarti and Visweswariah, 2020; Iatsenko et al., 2016)).

Our findings also uncovered that, despite releasing lower quantities of monomeric muropeptides than *E. coli*¹⁵, GanhM4 derived from *E. coli*^{MC4100} also possesses the capacity to initiate substantial local and systemic immune responses, including the rapid transcriptional induction of *AMP* genes within the nervous system. Although muropeptides derived from *E. coli*^{MC4100} are undetectable in the brain, they activate *AMP* transcription in this tissue. This suggests that even low levels of GanhM4 at the brain-circulation interface are sufficient to trigger NF- κ B activation. It is noteworthy that prior studies have illustrated how the activation of innate immunity in *Drosophila* neural cells is detrimental to the fly brain. Indeed, mutations in *dnr1* (defense repressor 1), a negative regulator of the IMD/NF- κ B pathway, or direct bacterial injection into the brain, lead to NF- κ B-dependent neurodegeneration due to the neurotoxic effects of AMPs (Cao et al., 2013). Mutations in intracellular negative regulators of the IMD/NF- κ B pathway predisposed flies to toxic levels of AMPs, resulting in early locomotor defects, extensive neurodegeneration, and reduced lifespan, a phenotype that could be rescued by suppressing immune activation in glial cells (Kounatidis et al., 2017). In our investigation, we identified perineurial glial cells as the principal contributors to AMP production in response to circulating muropeptides, indicating that gut-derived muropeptides trigger a localized inflammation of the BBB that correlates with neurological decline.

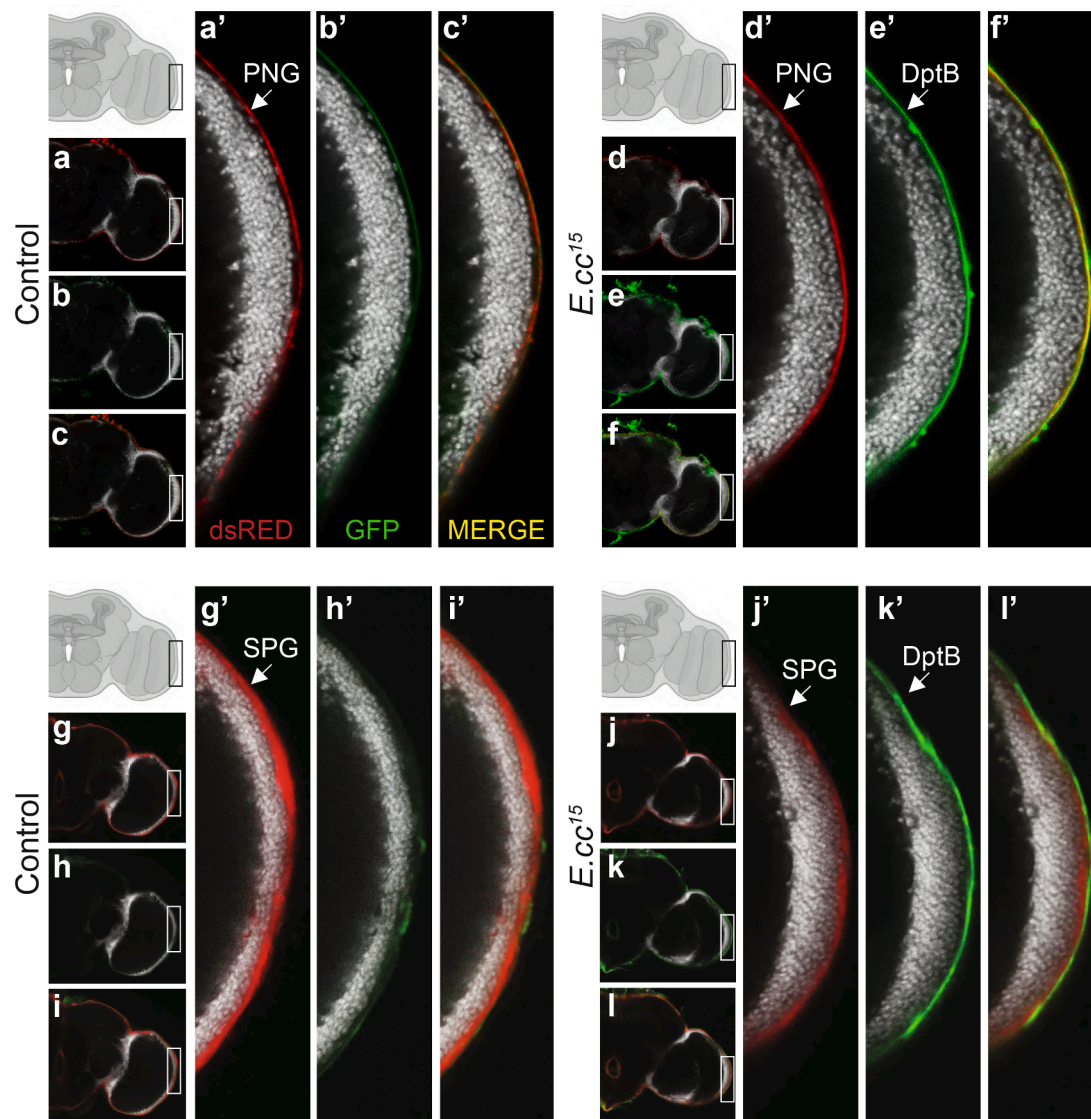
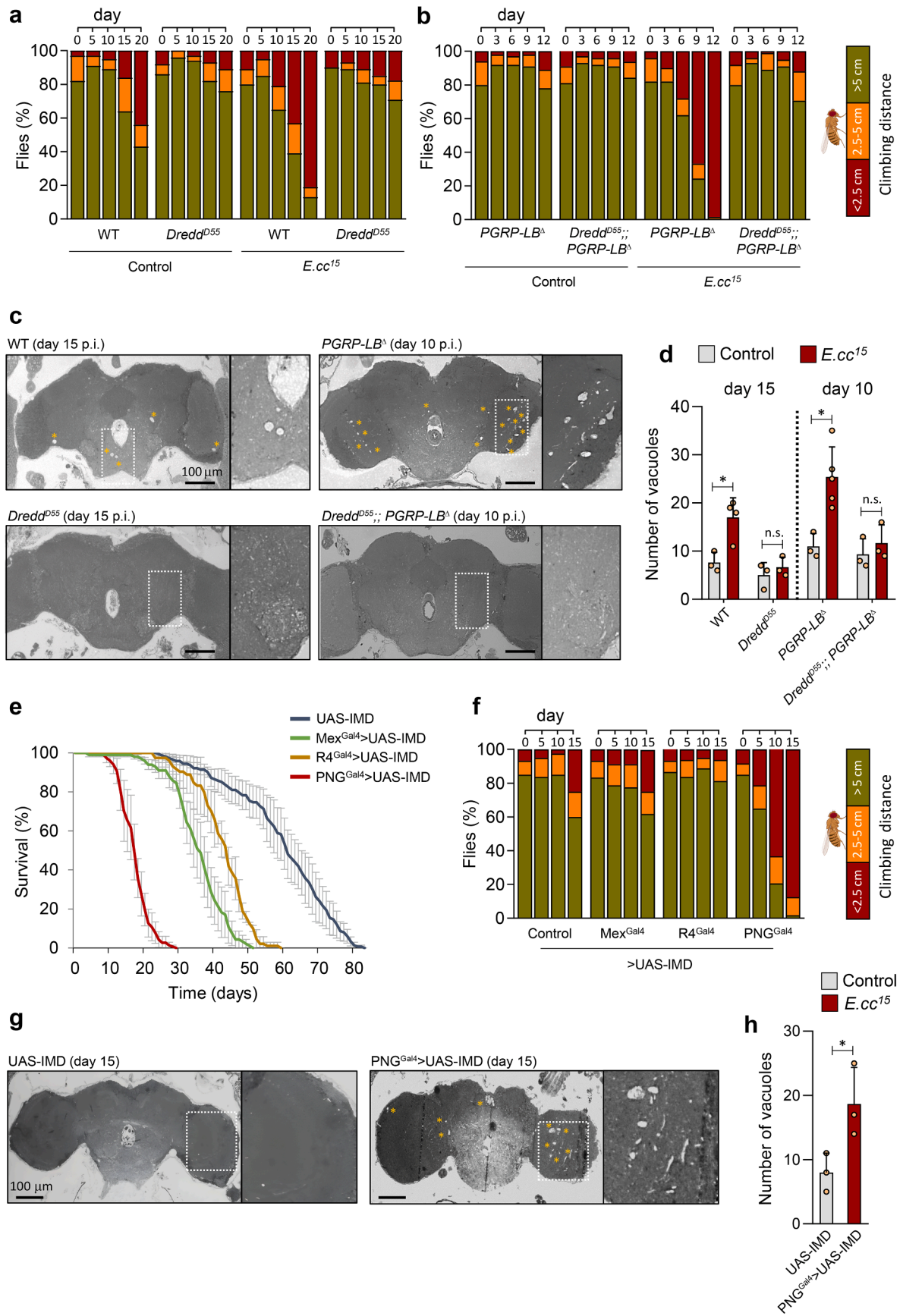


Fig. 8. *E. coli*¹⁵ ingestion induces expression of *Diptericin B* in the outer-cellular layer of the blood–brain barrier. (a–l) Representative single confocal images of brains from unchallenged (a–c and g–i) and *E. coli*¹⁵ orally infected (d–f and j–l) transgenic flies expressing the membrane bound reporter UAS-mcd8RFP under the control of the perineurial glial driver PNG^{Gal4} (a and d) or the subperineurial glial driver SPG^{Gal4} (g and j) along with the *Diptericin-GFP* inducible antimicrobial reporter (b, e, h and k). In all cases, TO-PRO-3 dye was used to counterstain the chromatin in nuclei. All three markers are shown in the merged image (c, f, i and l). (a'–l') Enlarged image of the optic lobe from respective boxed regions (a–l).

Considering the crucial evolutionary conserved role of the BBB in safeguarding the function of the CNS by regulating the exchange of ions, nutrients, and signaling molecules between the circulatory system and the nervous system (Featherstone, 2011; Graciela Delgado et al., 2018; Volkenhoff et al., 2015; Weiler et al., 2017), our results raise pertinent questions about the impact of circulating muropeptides and activation of the immune system on the homeostasis of the BBB and brain physiology.

In prior studies, we established that circulating PGN fragments can modulate the activity of a subset of octopaminergic neurons independently of antimicrobial peptides, which are traditionally recognized as the primary transcriptional targets of the IMD/NF- κ B pathway. While our transcriptomic analysis revealed the modulation of the expression of classical immune effectors and regulator genes associated with the IMD, Toll, and JAK/STAT signaling pathways, and are commonly observed in immunocompetent tissues or cells such as the fat body and enterocytes in response to bacterial infection (Buchon et al., 2009; Irving et al., 2001), it did not identify unique molecular signatures specific to CNS

cells, particularly neurons. The apparent minimal impact of gut bacterial infection on gene transcription in neurons raises consideration of at least two potential explanations. Firstly, it is conceivable that muropeptides present in the hemolymph are incapable of crossing the perineurial and subperineurial glial cells forming the two cell layers of the BBB (Schirmeier and Klämbt, 2015), thus failing to reach neurons. Alternatively, PGN fragments may enter into the brain, but not all internal neural cells may have the competence to respond to muropeptides by modulating gene expression. We are inclined to favor the latter hypothesis for several reasons. First, we have previously demonstrated that the inactivation of the cytosolic PRR *PGRP-LE* within a subset of octopaminergic neurons is sufficient to disrupt the influence of circulating PGN on oviposition behavior, implying that these neurons are accessible to PGN (Kurz et al., 2017). Second, our present findings indicate that at least *PGRP-LB* mRNA induction is dependent on the activation of the IMD/NF- κ B pathway in neurons but not in glial cells. Thus, it is conceivable that only a limited subset of neurons possesses the capability to sense



(caption on next page)

Fig. 9. Chronic *E. cc*¹⁵ intestinal infection and IMD/NF- κ B signaling in perineurial cells correlate with neurological decline. (a–b) Negative geotaxis assay performed in wild-type flies and *Dredd*^{D55} mutant flies (a), or *PGRP-LB*^d and *Dredd*^{D55}; *PGRP-LB*^d mutant flies (b) at specified days, under control conditions and *E. cc*¹⁵ infection. At day zero of the experiments, flies are aged 4–6 days. (c) Representative 5 μ m Epon sections (left) and magnified views of the boxed regions (right) from the midbrain of flies of specified genotypes at the indicated days post-oral infection (p.i.). Yellow stars highlight vacuoles (neurodegeneration). (d) Quantification of vacuole number observed in the brains of wild-type, *Dredd*^{D55}, *PGRP-LB*^d, and *Dredd*^{D55}; *PGRP-LB*^d flies at the indicated days under control conditions and post infection. Comparisons between selected conditions are shown (unpaired t-test, ns = not significant, and *p < 0.1). (e) Survival of control flies (UAS-IMD) and flies overexpressing IMD in enterocytes (*Mex*^{Gal4} > UAS-IMD), fat body cells (*R4*^{Gal4} > UAS-IMD) and perineurial glial cells (*PNG*^{Gal4} > UAS-IMD). The difference between control flies and those overexpressing IMD is significant (p < 0.001 respectively; one-sided log rank test). (f) Negative geotaxis assay performed in control flies and those overexpressing IMD at specified days. (g) Representative 5 μ m Epon sections (left) and magnified views of the boxed regions (right) from the midbrain of UAS-IMD and *PNG*^{Gal4} > UAS-IMD flies at day 15. (h) Quantification of vacuole number observed in the brains of UAS-IMD and *PNG*^{Gal4} > UAS-IMD flies at day 15 (unpaired t-test, *p < 0.1). (For interpretation of the references to colour in this figure legend, the reader is referred to the web version of this article.)

and respond to muropeptides by activating gene transcription, and such responses might be diluted in a comprehensive transcriptional analysis, like the one conducted in our study. In this regard, techniques such as *in situ* hybridization would offer the potential to precisely map the internal neurons expressing immune genes (Long et al., 2017). This would not only shed light on the neurons involved but also provide valuable insights into the spatial and cellular distribution of immune responses within the brain.

4. Materials and methods

4.1. *Drosophila melanogaster* strains and maintenance

The following *Drosophila melanogaster* strains were utilized in this study. The *w*¹¹¹⁸ strain (BL #6326) served as the reference control wild-type strain. *PGRP-LB* (Paredes et al., 2011) and *Fadd* mutant flies were generously provided by B. Lemaitre. The reference pan-glial repo^{Gal4} (BL#7415) and pan-neuronal elav^{Gal4} (BL#8760) drivers were obtained from the Bloomington *Drosophila* Stock Center. Gal4 enhancers for different subtypes of glial cells, namely NP6293 (perineurial glia, *PNG*^{Gal4}, DGRC#103–953), NP6520 (ensheathing glia, *EG*^{Gal4}, DGRC#105–240), NP2222 (cortex glia, *CG*^{Gal4}, DGRC#112–830), and NP3233 (astrocyte-like glia, *AG*^{Gal4}, DGRC#103–953), were generated by the NP consortium and obtained from the KYOTO Stock Center. The RC54C07 strain (subperineurial glia, *SPN*^{Gal4}, BL#50472) was generated by the Rubin Laboratory at Janelia Farm, and the 9-137^{Gal4} enhancer, driving expression in both layers of the BBB, was provided by Roland Bainton (DeSalvo et al., 2014). The Fat Body *R4*^{Gal4} driver (BL#33832) was obtained from the Bloomington *Drosophila* Stock Center. The enterocyte driver *Mex*^{Gal4} (Phillips and Thomas, 2006) and the UAS-IMD strain (Georgel et al., 2001) were kindly provided by Yixian Zheng and François Leulier, respectively. The UAS-*PGRP-LB*^{RC} strain was described elsewhere (Charroux et al., 2018). The membrane-bound reporter UAS-mcd8RFP (BL#27398) is from the Bloomington *Drosophila* Stock Center. The Inducible *Attacin-A-GFP*, *Metchnikowin-GFP* and *Diptericin-B-GFP* antimicrobial reporter flies were obtained from B. Lemaitre (Tzou et al., 2000).

Flies were reared at 25 °C on a yeast/cornmeal medium in incubators controlled for a 12 h light/12 h dark cycle. For the preparation of 1 L of food, 8.2 g of agar (VWR, cat. #20768.361), 80 g of cornmeal flour (Westhove, Farigel maize H1), and 80 g of yeast extract (VWR, cat. #24979.413) were cooked for 10 min in boiling water. After the food had cooled down, 5.2 g of Methylparaben sodium salt (MERCK, cat #106756) and 4 ml of 99 % propionic acid (CARLOERBA, cat. #409553) were added. For antibiotic (ATB) treatment, the standard medium was supplemented with Ampicillin, Kanamycin, Tetracycline, and Erythromycin at final concentrations of 50 μ g/ml.

4.2. Bacterial oral infection of adult flies

The bacterial strains utilized in this study included *Erwinia carotovora carotovora* 15 2141 (*E. cc*¹⁵) and *Escherichia coli* (*E. c*) MC4100, MC1061, and MG1655. *E. cc*¹⁵ was cultured in Luria-Bertani medium (LB) at 30 °C, while *E. c* strains were cultured at 37 °C overnight. Subsequently,

bacterial cultures were centrifuged at 2500 g for 20 min at room temperature. The bacterial cells were then serially diluted in LB medium, and their concentrations were determined by measuring optical density (OD) at 600 nm.

For the purpose of oral infection and subsequent analysis, 4–6 days old female flies were reared at 25 °C in the presence of ATB in their food. Twenty-four hours prior to infection, female flies were transferred to vials without antibiotics and then placed in fly vials containing food contaminated with either *E. cc*¹⁵ or *E. c*^{M4100}. The bacterial food solution was prepared by mixing a pellet of an overnight bacterial culture (OD = 200) with a 5 % sucrose solution (50/50 ratio). This mixture was applied to a filter disk, covering the entire agar surface of the fly vial.

4.3. Hemolymph collection from adult flies

To obtain hemolymph samples, unchallenged and orally infected flies with *E. c*^{M4100} or *E. cc*¹⁵ (n = 60 per sample) were anesthetized using CO₂, and their heads were excised using a razor blade. The decapitated fly bodies were then rapidly transferred into perforated 0.5 ml Eppendorf tubes and placed inside a 1.5 ml Eppendorf collection tube. Hemolymph was then extracted via centrifugation for 5 min at 5000 rpm at 4 °C. The collection tubes containing the hemolymph were immediately frozen in liquid nitrogen and subsequently stored at –80 °C until further analysis.

4.4. Ex-Vivo brain cultures

Brains (n = 20 per sample) from 4–6 days old female flies were dissected in cold phosphate-buffered saline (PBS) and rapidly transferred to Schneider insect cell-culture medium (Sigma) complemented with 5 % fetal bovine serum (FBS) and supplemented with penicillin (5000 units/ml), and streptomycin (5 mg/ml). *Ex-vivo* cultures were then incubated at 25 °C for 16 h, with or without peptidoglycan purified from *E. coli* (InvivoGen, #14C14-MM, CA, USA), or GanhM4 purified from *E. cc*¹⁵, before RNA extraction.

4.5. Quantitative Real-Time PCR

RNA from whole female flies (n = 5 per sample) and dissected guts, fat bodies, and brains (n = 20 per sample) was extracted using the RNeasy Mini Kit (QIAGEN, cat. #74106). Quantitative real-time PCR, TaqMan, and SYBR Green analyses were performed as previously described (Charroux et al., 2018). The mRNA levels detected were normalized to control *rp49* mRNA values. Normalized data were used to quantify the relative levels of a given mRNA based on cycling threshold analysis (Δ Ct). Results are presented as the average and standard deviation of a minimum of three independent experiments. Statistical analyses were conducted using unpaired t-tests within Prism (GraphPad Software).

4.6. qRT-PCR primers

Primers used for qRT-PCR are listed in the table below:

Gene	Forward primer	Reverse primer
<i>rp49</i>	TGCTAAGCTGTCCGCACAAATGG	TGCGCTTGTTCGATCCGTAAC
<i>AttA</i>	CCCGGAGTGAAGGATG	GTTGCTGTCCGTCAAG
<i>AttB</i>	AGCAACTTCCCAGGAATCGG	GTAGTAGCACGATTGGGCGA
<i>AttC</i>	TGCCCGATTGGACCTAAGC	GCCTATGGGTTTTGGTCAGTTC
<i>AttD</i>	GTCCTAGGGTTCCTCAG	GCCGAAATCGGACTTG
<i>CecA1</i>	AAGCTGGGTGGCTGAAGAAA	TGTTGAGCGATTCCCAGTCC
<i>CecA2</i>	TGGCCATCACCATTTGGACAA	CCTGTTGAGCGATTCCCAGT
<i>CecC</i>	GCATTGGACAATCGGAAGCC	TGCCGAATCCCAGTCCCTT
<i>CG45045</i>	GCTGCCTGCAAAAATCACGA	GCATAGGGATTGCAAGCGGG
<i>DptB</i>	GCTGCGCAATCGCTTCTACT	TGGTGGAGTGGGCTTCATG
<i>GNBP-like3</i>	TGCCGAATTCCCAGTCCCTT	GTTCCGGTTGGGATAAAGTCCA
<i>Listericin</i>	AACAGTACTGGTGTTCGCC	ATCATCGATTCCCAGTGTG
<i>Mtk</i>	GATGCAACTTAATCTTGGAGCG	TTAATAAAATTTGGACCCGGTCTTGGTTGG
<i>PGRP-LB</i>	TGATCGGAGATTGGAGAACC	TAGGCAGGGTCAATGTAGCC
<i>PGRP-LF</i>	GGATGCGAACAAGAGGATGT	GGATGCGAACAAGAGGATGT
<i>PGRP-SA</i>	ACGGGCATAGCTTTATCGG	TAATCCTCGCTCAGCTACC
<i>PGRP-SB1</i>	TCAACGGCAATAGTTTTGTGGC	CTGCTGCGTGGTTCAATCTG
<i>PGRP-SC2</i>	CCACACCGCTGGAAACTACT	CCGCCGATCAGGAAGTTGTA
<i>PGRP-SD</i>	GACAGCATGGAAACTCCCTTG	GTTTTGCAGATTTGCAATGTGC
<i>TotA</i>	TTCCGACGAAGATCGTGAGG	CTGGGTGCTATTGATTTGGAGT
<i>TotC</i>	GCCTCCATTTCTACTATGCC	TCCCTTTCCTCGTCAGAATAGC
<i>TotM</i>	TCACAGAAAAACAGCGCCTAT	ATCGTAGAAAGTGACCAGGCT

4.7. Immunohistochemistry and imaging

Dissected brains from adult flies of the specified genotypes were fixed on ice for 10 min in 4 % paraformaldehyde and subsequently rinsed for 10 min with cold PBS. Following fixation, brains were incubated for 1 h at room temperature with agitation in blocking buffer (1X PBS / 2.5 % BSA / 0.3 % Triton X-100). For immunostaining, brains were incubated overnight at 4 °C with primary antibodies: anti-GFP (Aves Labs., catalogue No. GFP-1020, 1:1000 dilution) in combination with anti-RFP (ChromoTek, catalogue No. 5F8, 1:1000 dilution), or anti-elav (DSHB, catalogue No. 7E8A10, 1:50 dilution). Subsequently, brains were washed three times for 10 min at room temperature in blocking buffer. Next, brains were incubated for 2 h with secondary antibodies: Alexa Fluor 488 (Jackson ImmunoResearch, No. 703 545 155, 1:500 dilution) and Cyanine3 (Jackson ImmunoResearch, No. 712 165 153, 1:500 dilution), followed by three washes of 10 min at room temperature in blocking buffer. Finally, the brains were stained with the TO-PRO-3 nucleic acid marker in PBS before being mounted in Vectashield fluorescent mounting medium (Vector Laboratories, CA, USA). Images were captured using an LSM 780 Zeiss confocal microscope.

4.8. Experimental procedure for RNAseq analysis

The RNAseq analysis encompassed nine samples in total, consisting of three sample groups: brains from non-infected wild-type flies and brains from wild-type and *PGRP-LB* mutant flies orally infected with *E. cc¹⁵* for 16 h. Each sample consisted of 20 brains isolated from adult females aged 4–6 days. RNA was extracted from each sample using the RNeasy Mini Kit (QIAGEN, cat. #74106). The extracted RNA samples were then sent to the GenomEast platform, located in Strasbourg, France, for further analysis. RNA-Seq libraries were generated from 250 ng of total RNA using the TruSeq Stranded mRNA Library Prep Kit and TruSeq RNA Single Indexes kits A and B (Illumina, San Diego, CA), following the manufacturer's instructions. During this process, only polyA RNAs were sequenced to focus on the mature messenger RNA fraction. The quality and quantity of the generated cDNA libraries were assessed using capillary electrophoresis. The sequencing was performed using HiSeq4000, producing 2x100 base pair reads, with all samples run in one lane. Image analysis and base calling were performed using RTA 2.7.3 and bcl2fastq 2.17.1.14, converting the raw data from the sequencer into a format ready for downstream bioinformatic analysis.

4.9. Bioinformatic analysis of RNAseq data

The RNAseq data were subjected to a series of bioinformatic analyses. Quality control of the sequenced reads was executed using HTSeq, with the removal of the first 18 nucleotides of each read. Subsequently, the reads were aligned to the *Drosophila melanogaster* reference genome (dmel6.31, FlyBase) utilizing HISAT2 version 2. Gene expression quantification was carried out with the featureCounts function from the Rsubread package. Normalization of read counts and the analysis of differential gene expression were conducted using the DESeq2 package via the SARTools pipeline. All high-throughput sequencing data generated in this study have been deposited in Gene Expression Omnibus (GEO) and are available under the accession number GSE255079. Raw data and processed files of the RNA-seq analysis can be found in [Supplemental Data 1-4](#). For functional annotation and pathway enrichment analyses, DAVID was employed for Gene Ontology (GO) term analysis, and G:Profiler was used for KEGG pathway analysis. Finally, heatmaps for visual exploration of gene expression patterns were generated using the pheatmap package in R.

4.10. LC-HRMS sample preparation

Whole flies and biological specimens (heads, head capsules, brains, guts, carcasses and hemolymph) were immersed in 500 µL of pure water (Invitrogen) to obtain homogenates through sonication (Bioblock Vibracell 75043) at 4 °C. Two hundred microliters of each sample were freeze-dried and resuspended with an aqueous solution of M3K, as an internal standard, at 0.5 µM before liquid–liquid extraction. The sample extraction was inspired by the sequential precipitation and delipidation protocol published by Li *et al.* (Li *et al.*, 2020). A single-phase solvent system Diisopropyl ether/methanol/water (5:3:1, v/v) and a two-phase solvent system Diisopropyl ether/methanol/water (5:1:1, v/v) were applied on homogenates of *Drosophila* organs. After proteins precipitation, the lower phase from the delipidation step was collected and lyophilized under vacuum (SpeedVacTM, Thermo Fisher Scientific) for LC-HRMS analysis.

4.11. LC-HRMS analyses

LC-HRMS analyses were performed using an Ultimate 3000 Ultra High-Performance Chromatography system (UHPLC; Dionex / Thermo Fisher Scientific) coupled to a Q Exactive Orbitrap mass spectrometer (Q Exactive Focus; Thermo Fisher Scientific). The extract samples were re-

dissolved in 50 μ l of murabutide (external standard at 100 nM) with 0.1 % Formic acid (FA) and separated on a Hypersil GOLD aQ C18 analytical column (150 x 2.1 mm, 1.9 μ m) with mobile phase A (0.1 % FA) and mobile phase B (AcN containing 0.1 % FA). After injection of 10 μ l of sample, the elution consisted to a nonlinear two-step gradient from 0 to 80 % of phase over 32 min with a mobile phase flow rate of 200 μ l/min. The column was flushed for 10 min with 80 % of phase B before letting the system equilibrate for 8 min with 100 % of phase A.

MS analyses were performed in the positive ion mode, and sequential MS2 experiments were carried out using data-dependent acquisition method. The MS detection was performed from m/z 120 to 1,800 using a resolution set at 70,000 at m/z 200 (full width at half-maximum, FWHM). MS/MS spectra were acquired on a “Top 3” data-dependent mode using the following parameters: resolution 17,500; Automatic Gain Control (AGC) 1×10^5 ions with a maximum ion injection time of 50 ms. A normalized collision energy (NCE) of 25 % was used for the fragmentation of mucopeptides. XCalibur 4.0 software from Thermo Fisher Scientific was used to control the instrument and for data processing.

4.12. Lifespan and locomotion assays

To conduct survival assays during chronic infection, 4–6-day-old flies reared at 25 °C of each indicated genotype were exposed to a fresh solution of *Ecc*¹⁵ (OD = 200) every 2 days, combined with a 5 % sucrose solution (50/50). Survival analyses in the absence of infection were performed in vials containing an LB medium solution and a 5 % sucrose solution (50/50) in the presence of ATB. The assessment of deceased flies occurred at a designated time once a day. Each survival assay utilized a minimum of three vials, each containing 25 flies. The experiments were independently replicated at least twice. Statistical analyses used a one-sided log-rank test within Prism (GraphPad software).

For the locomotor activity assessment, a climbing assay was designed to quantify spontaneous locomotion driven by *Drosophila*'s inherent negative geotactic behavior. This assay was employed to evaluate the locomotor activity of groups comprising 25 adult flies for each specified genotype. The motor function response was assessed daily in plastic rearing vials (2.5 cm in diameter and 9.5 cm in height) by scoring the vertical climbing distance (<2.5 cm, 2.5–5 cm, or > 5 cm) for a duration of 20 s at room temperature when flies were gently tapped to the bottom of the vial. Three independent replicates were averaged for each condition.

4.13. Brain histology and neurodegeneration assessment

Fly heads were severed and immersed in fixative (2.5 % glutaraldehyde and 2.5 % paraformaldehyde in 0.1 M cacodylate Buffer, pH 7.4) overnight at 4 °C. Subsequently, heads were post-fixed with 1 % osmium tetroxide in 100 mM cacodylate buffer (pH 7.0) for 2 h at 4 °C before undergoing dehydration and embedding in Epon. Embedded heads were sectioned at a thickness of 5 μ m and stained with Toluidine blue (0.1 % in 1 % sodium borate). Imaging of the sections was conducted using a light microscope under white light. To evaluate neurodegeneration, the number of vacuoles that had developed in the neuropil of the central brain was scored in ten consecutive sections per head. Three to five heads were used for each histological experiment.

5. Data availability

The numerical data and statistical analysis supporting the findings of this study are available within the [supplementary materials \(Supplemental Data 5-6\)](#).

6. Resource availability

6.1. Lead contacts and materials availability

Further information and requests for resources and reagents reported in this paper should be directed to and will be fulfilled by the Lead Contacts, Julien Royet (julien.royet@univ-amu.fr) and Olivier Zugasti (olivier.zugasti@univ-amu.fr).

CRediT authorship contribution statement

Florent Fioriti: Conceptualization, Investigation, Formal analysis. **Aline Rifflet:** Conceptualization, Investigation, Formal analysis. **Ivo Gomperts Boneca:** Funding acquisition, Supervision, Conceptualization. **Olivier Zugasti:** Conceptualization, Investigation, Formal analysis, Supervision, Writing – review & editing, Writing – original draft, Data curation. **Julien Royet:** Writing – review & editing, Writing – original draft, Supervision, Funding acquisition, Formal analysis, Data curation, Conceptualization..

Declaration of Competing Interest

The authors declare that they have no known competing financial interests or personal relationships that could have appeared to influence the work reported in this paper.

Data availability

Data will be made available on request.

Acknowledgments

We thank Annelise Viallat-Lieutaud, Raphaël Tavignot, Romane Milleville, Martina Montanari, and Olivier Danot for their technical assistance, and extend our appreciation to Aïcha Aouane from the Marseille Institute of Development Biology (IBDM) microscopy platform. This work was supported by CNRS, ANR Peptimet (ANR-18-CE15-0018), Equipe Fondation pour la Recherche Médicale (EQU201903007783), and l'Institut Universitaire de France to J.R., as well as by the ANR Pepneuron (ANR-21-CE16-0027).

Appendix A. Supplementary data

Supplementary data to this article can be found online at <https://doi.org/10.1016/j.bbi.2024.05.009>.

References

- Agus, A., Clément, K., Sokol, H., 2021. Gut microbiota-derived metabolites as central regulators in metabolic disorders. *Gut* 70, 1174–1182. <https://doi.org/10.1136/gutjnl-2020-323071>.
- Ali, Y.O., Escala, W., Ruan, K., Zhai, R.G., 2011. Assaying locomotor, learning, and memory deficits in *Drosophila* models of neurodegeneration. *J vis Exp* 2504. <https://doi.org/10.3791/2504>.
- Arentsen, T., Qian, Y., Gkotsis, S., Femenia, T., Wang, T., Udekwi, K., Forssberg, H., Diaz, H.R., 2017. The bacterial peptidoglycan-sensing molecule Pglyrp2 modulates brain development and behavior. *Mol Psychiatry* 22, 257–266. <https://doi.org/10.1038/mp.2016.182>.
- Basset, A., Khush, R.S., Braun, A., Gardan, L., Boccard, F., Hoffmann, J.A., Lemaitre, B., 2000. The phytopathogenic bacteria *Erwinia carotovora* infects *Drosophila* and activates an immune response. *Proc Natl Acad Sci U S A* 97, 3376–3381.
- Basset, A., Tzou, P., Lemaitre, B., Boccard, F., 2003. A single gene that promotes interaction of a phytopathogenic bacterium with its insect vector, *Drosophila melanogaster*. *EMBO Rep* 4, 205–209. <https://doi.org/10.1038/sj.embor.embor730>.
- Bharadwaj, R., Lusi, C.F., Mashayekh, S., Nagar, A., Subbarao, M., Kane, G.L., Wodzanowski, K.A., Brown, A.R., Okuda, K., Monahan, A., Paik, D., Nandy, A., Anonick, M.V., Goldman, W.E., Kanneganti, T.-D., Orzalli, M.H., Grimes, C.L., Atukorale, P.U., Silverman, N., 2023. Methotrexate suppresses psoriatic skin inflammation by inhibiting mucopeptide transporter SLC46A2 activity. *Immunity* 56, 998–1012.e8. <https://doi.org/10.1016/j.immuni.2023.04.001>.

- Bischoff, V., Vignal, C., Duvic, B., Boneca, I.G., Hoffmann, J.A., Royet, J., 2006. Downregulation of the *Drosophila* Immune Response by Peptidoglycan-Recognition Proteins SC1 and SC2. *PLoS Pathogens* 2, e14.
- Biswas, A., Kobayashi, K.S., 2013. Regulation of intestinal microbiota by the NLR protein family. *Int Immunol* 25, 207–214. <https://doi.org/10.1093/intimm/dxs116>.
- Bosco-Drayon, V., Poidevin, M., Boneca, I.G., Narbonne-Reveau, K., Royet, J., Charroux, B., 2012. Peptidoglycan sensing by the receptor PGRP-LE in the *Drosophila* gut induces immune responses to infectious bacteria and tolerance to microbiota. *Cell Host Microbe* 12, 153–165. <https://doi.org/10.1016/j.chom.2012.06.002>.
- Branton, W.G., Lu, J.Q., Surette, M.G., Holt, R.A., Lind, J., Laman, J.D., Power, C., 2016. Brain microbiota disruption within inflammatory demyelinating lesions in multiple sclerosis. *Sci Rep* 6, 37344. <https://doi.org/10.1038/srep37344>.
- Bu, H.-F., Wang, X., Tang, Y., Koti, V., Tan, X.-D., 2010. Toll-like receptor 2-mediated peptidoglycan uptake by immature intestinal epithelial cells from apical side and exosome-associated transcellular transcytosis. *J Cell Physiol* 222, 658–668. <https://doi.org/10.1002/jcp.21985>.
- Buchon, N., Broderick, N.A., Poidevin, M., Pradervand, S., Lemaitre, B., 2009. *Drosophila* intestinal response to bacterial infection: activation of host defense and stem cell proliferation. *Cell Host Microbe* 5, 200–211. <https://doi.org/10.1016/j.chom.2009.01.003>.
- Buchon, N., Broderick, N.A., Lemaitre, B., 2013. Gut homeostasis in a microbial world: insights from *Drosophila melanogaster*. *Nat Rev Microbiol* 11, 615–626. <https://doi.org/10.1038/nrmicro3074>.
- Cao, Y., Chtarbanova, S., Petersen, A.J., Ganetzky, B., 2013. Dnr1 mutations cause neurodegeneration in *Drosophila* by activating the innate immune response in the brain. *Proc Natl Acad Sci U S A* 110, E1752. <https://doi.org/10.1073/pnas.1306220110>.
- Chakrabarti, S., Visweswariah, S.S., 2020. Intramacrophage ROS Primes the Innate Immune System via JAK/STAT and Toll Activation. *Cell Rep* 33, 108368. <https://doi.org/10.1016/j.celrep.2020.108368>.
- Chang, C.-I., Chelliah, Y., Borek, D., Mengin-Lecreux, D., Deisenhofer, J., 2006. Structure of tracheal cytotoxin in complex with a heterodimeric pattern-recognition receptor. *Science* 311, 1761–1764. <https://doi.org/10.1126/science.1123056>.
- Charroux, B., Capo, F., Kurz, C.L., Peslier, S., Chaduli, D., Viallat-Lieutaud, A., Royet, J., 2018. Cytosolic and Secreted Peptidoglycan-Degrading Enzymes in *Drosophila* Respectively Control Local and Systemic Immune Responses to Microbiota. *Cell Host Microbe* 23, 215–228.e4. <https://doi.org/10.1016/j.chom.2017.12.007>.
- Clarke, T.B., Davis, K.M., Lysenko, E.S., Zhou, A.Y., Yu, Y., Weiser, J.N., 2010. Recognition of peptidoglycan from the microbiota by Nod1 enhances systemic innate immunity. *Nat Med* 16, 228–231. <https://doi.org/10.1038/nm.2087>.
- Clemmons, A.W., Lindsay, S.A., Wasserman, S.A., 2015. An effector Peptide family required for *Drosophila* toll-mediated immunity. *PLoS Pathogens* 11, e1004876.
- Corby-Harris, V., Pontaroli, A.C., Shimkets, L.J., Bennetzen, J.L., Habel, K.E., Promislow, D.E.L., 2007. Geographical distribution and diversity of bacteria associated with natural populations of *Drosophila melanogaster*. *Appl Environ Microbiol* 73, 3470–3479. <https://doi.org/10.1128/aem.02120-06>.
- DeSalvo, M.K., Hindle, S.J., Rusan, Z.M., Orng, S., Eddison, M., Halliwill, K., Bainton, R. J., 2014. The *Drosophila* surface glia transcriptome: evolutionary conserved blood-brain barrier processes. *Front Neurosci* 8, 346. <https://doi.org/10.3389/fnins.2014.00346>.
- Dushay, M.S., Asling, B., Hultmark, D., 1996. Origins of immunity: Relish, a compound Rel-like gene in the antibacterial defense of *Drosophila*. *Proc Natl Acad Sci U S A* 93, 10343–10347. <https://doi.org/10.1073/pnas.93.19.10343>.
- Fan, Y., Pedersen, O., 2021. Gut microbiota in human metabolic health and disease. *Nat Rev Microbiol* 19, 55–71. <https://doi.org/10.1038/s41579-020-0433-9>.
- Featherstone, D.E., 2011. Glial solute carrier transporters in *Drosophila* and mice. *Glia* 59, 1351–1363. <https://doi.org/10.1002/glia.21085>.
- Gabanyi, I., Lepousez, G., Wheeler, R., Vieites-Prado, A., Nissant, A., Chevalier, G., Wagner, S., Moigneu, C., Dulauroy, S., Hicham, S., Polomack, B., Verny, F., Rosenstiel, P., Renier, N., Boneca, I.G., Eberl, G., Lledo, P.-M., 2022. Bacterial sensing via neuronal Nod2 regulates appetite and body temperature. *Science* 376, eabj3986. <https://doi.org/10.1126/science.abj3986>.
- Gendrin, M., Welchman, D.P., Poidevin, M., Hervé, M., Lemaitre, B., 2009. Long-range activation of systemic immunity through peptidoglycan diffusion in *Drosophila*. *PLoS Pathogens* 5, e1000694.
- Georgel, P., Naitza, S., Kappler, C., Ferrandon, D., Zachary, D., Swimmer, C., Kopczynski, C., Duyk, G., Reichhart, J.M., Hoffmann, J.A., 2001. *Drosophila* immune deficiency (IMD) is a death domain protein that activates antibacterial defense and can promote apoptosis. *Dev Cell* 1, 503–514. [https://doi.org/10.1016/s1534-5807\(01\)00059-4](https://doi.org/10.1016/s1534-5807(01)00059-4).
- Girardin, S.E., Boneca, I.G., Carneiro, L.A.M., Antignac, A., Jéhanno, M., Viala, J., Tedin, K., Taha, M.-K., Labigne, A., Zähringer, U., Coyle, A.J., DiStefano, P.S., Bertin, J., Sansonetti, P.J., Philpott, D.J., 2003a. Nod1 Detects a Unique Muropeptide from Gram-Negative Bacterial Peptidoglycan. *Science* 300, 1584–1587. <https://doi.org/10.1126/science.1084677>.
- Girardin, S.E., Boneca, I.G., Viala, J., Chamaillard, M., Labigne, A., Thomas, G., Philpott, D.J., Sansonetti, P.J., 2003b. Nod2 Is a General Sensor of Peptidoglycan through Muramyl Dipeptide (MDP) Detection *. *Journal of Biological Chemistry* 278, 8869–8872. <https://doi.org/10.1074/jbc.C200651200>.
- Girardin, S.E., Philpott, D.J., 2004. Mini-review: The role of peptidoglycan recognition in innate immunity. *European Journal of Immunology* 34, 1777–1782. <https://doi.org/10.1002/eji.200425095>.
- Gottar, M., Gobert, V., Michel, T., Belvin, M., Duyk, G., Hoffmann, J.A., Ferrandon, D., Royet, J., 2002. The *Drosophila* immune response against Gram-negative bacteria is mediated by a peptidoglycan recognition protein. *Nature* 416, 640–644. <https://doi.org/10.1038/nature734>.
- Graciela Delgado, M., Oliva, C., Lopez, E., Ibacache, A., Galaz, A., Delgado, R., Felipe Barros, L., Sierralta, J., 2018. Chaski, a novel *Drosophila* lactate/pyruvate transporter required in glia cells for survival under nutritional stress. *Sci Rep* 8, 1186. <https://doi.org/10.1038/s41598-018-19595-5>.
- Guo, S., Al-Sadi, R., Said, H.M., Ma, T.Y., 2013. Lipopolysaccharide causes an increase in intestinal tight junction permeability in vitro and in vivo by inducing enterocyte membrane expression and localization of TLR-4 and CD14. *Am J Pathol* 182, 375–387. <https://doi.org/10.1016/j.ajpath.2012.10.014>.
- Guo, S., Nighot, M., Al-Sadi, R., Alhmoud, T., Nighot, P., Ma, T.Y., 2015. Lipopolysaccharide Regulation of Intestinal Tight Junction Permeability Is Mediated by TLR4 Signal Transduction Pathway Activation of FAK and MyD88. *The Journal of Immunology* 195, 4999–5010. <https://doi.org/10.4049/jimmunol.1402598>.
- Hu, Y., Flockhart, I., Vinayagam, A., Bergwitz, C., Berger, B., Perrimon, N., Mohr, S.E., 2011. An integrative approach to ortholog prediction for disease-focused and other functional studies. *BMC Bioinformatics* 12, 357. <https://doi.org/10.1186/1471-2105-12-357>.
- Humann, J., Mann, B., Gao, G., Moresco, P., Ramahi, J., Loh, L.N., Farr, A., Hu, Y., Durick-Eder, K., Fillon, S.A., Smeyne, R.J., Tuomanen, E.I., 2016. Bacterial Peptidoglycan Traverses the Placenta to Induce Fetal Neuroproliferation and Aberrant Postnatal Behavior. *Cell Host Microbe* 19, 388–399. <https://doi.org/10.1016/j.chom.2016.02.009>.
- Iatsenko, I., Kondo, S., Mengin-Lecreux, D., Lemaitre, B., 2016. PGRP-SD, an Extracellular Pattern-Recognition Receptor, Enhances Peptidoglycan-Mediated Activation of the *Drosophila* Imd Pathway. *Immunity* 45, 1013–1023. <https://doi.org/10.1016/j.immuni.2016.10.029>.
- Irazoki, O., Hernandez, S.B., Cava, F., 2019. Peptidoglycan Muropeptides: Release, Perception, and Functions as Signaling Molecules. *Front Microbiol* 10, 500. <https://doi.org/10.3389/fmicb.2019.00500>.
- Irving, P., Troxler, L., Heuer, T.S., Belvin, M., Kopczynski, C., Reichhart, J.-M., Hoffmann, J.A., Hetru, C., 2001. A genome-wide analysis of immune responses in *Drosophila*. *Proc Natl Acad Sci U S A* 98, 15119–15124. <https://doi.org/10.1073/pnas.261573998>.
- Janeway, C.A., Medzhitov, R., 2002. Innate immune recognition. *Annu Rev Immunol* 20, 197–216. <https://doi.org/10.1146/annurev.immunol.20.083001.084359>.
- Joshi M, Viallat-Lieutaud A, Royet J. 2023. Role of Rab5 early endosomes in regulating *Drosophila* gut antibacterial response. *iScience* 26:107335. doi:10.1016/j.isci.2023.107335.
- Kamareddine, L., Najjar, H., Sohail, M.U., Abdulkader, H., Al-Asmakh, M., 2020. The Microbiota and Gut-Related Disorders: Insights from Animal Models. *Cells* 9, 2401. <https://doi.org/10.3390/cells9112401>.
- Kaneko, T., Goldman, W.E., Mellroth, P., Steiner, H., Fukase, K., Kusumoto, S., Harley, W., Fox, A., Golenbock, D., Silverman, N., 2004. Monomeric and polymeric gram-negative peptidoglycan but not purified LPS stimulate the *Drosophila* IMD pathway. *Immunity* 20, 637–649. [https://doi.org/10.1016/s1074-7613\(04\)00104-9](https://doi.org/10.1016/s1074-7613(04)00104-9).
- Kawai, T., Akira, S., 2009. The roles of TLRs, RLRs and NLRs in pathogen recognition. *Int Immunol* 21, 317–337. <https://doi.org/10.1093/intimm/dxp017>.
- Kleino, A., Myllymäki, H., Kallio, J., Vanha-aho, L.-M., Oksanen, K., Ulvila, J., Hultmark, D., Valanne, S., Rämert, M., 2008. Pirk is a negative regulator of the *Drosophila* Imd pathway. *J Immunol* 180, 5413–5422. <https://doi.org/10.4049/jimmunol.180.8.5413>.
- Kounatidis, I., Chtarbanova, S., Cao, Y., Hayne, M., Jayanth, D., Ganetzky, B., Ligoxygakis, P., 2017. NF-κB Immunity in the Brain Determines Fly Lifespan in Healthy Aging and Age-Related Neurodegeneration. *Cell Rep* 19, 836–848. <https://doi.org/10.1016/j.celrep.2017.04.007>.
- Kremer, M.C., Jung, C., Batelli, S., Rubin, G.M., Gaul, U., 2017. The glia of the adult *Drosophila* nervous system. *Glia* 65, 606–638. <https://doi.org/10.1002/glia.23115>.
- Kurz, C.L., Charroux, B., Chaduli, D., Viallat-Lieutaud, A., Royet, J., 2017. Peptidoglycan Sensing by Octopaminergic Neurons Modulates *Drosophila* Oviposition. *eLife* 6: e21937. <https://doi.org/10.7554/eLife.21937>.
- Laman JD, Hart BA t, Power C, Dziarski R. 2020. Bacterial Peptidoglycan as a Driver of Chronic Brain Inflammation. *Trends in Molecular Medicine* 26:670–682. doi: 10.1016/j.molmed.2019.11.006.
- Lemaitre, B., Nicolas, E., Michaut, L., Reichhart, J.M., Hoffmann, J.A., 1996. The dorsoventral regulatory gene cassette *spätzle/Toll/cactus* controls the potent antifungal response in *Drosophila* adults. *Cell* 86, 973–983. [https://doi.org/10.1016/s0092-8674\(00\)80172-5](https://doi.org/10.1016/s0092-8674(00)80172-5).
- Leulier, F., Vidal, S., Saigo, K., Ueda, R., Lemaitre, B., 2002. Inducible expression of double-stranded RNA reveals a role for dFADD in the regulation of the antibacterial response in *Drosophila* adults. *Curr Biol* 12, 996–1000. [https://doi.org/10.1016/s0960-9822\(02\)00873-4](https://doi.org/10.1016/s0960-9822(02)00873-4).
- Leulier, F., Parquet, C., Pili-Floury, S., Ryu, J.-H., Caroff, M., Lee, W.-J., Mengin-Lecreux, D., Lemaitre, B., 2003. The *Drosophila* immune system detects bacteria through specific peptidoglycan recognition. *Nat Immunol* 4, 478–484. <https://doi.org/10.1038/ni922>.
- Li, N., Zhou, Y., Wang, J., Niu, L., Zhang, Q., Sun, L., Ding, X., Guo, X., Xie, Z., Zhu, N., Zhang, M., Chen, X., Cai, T., Yang, F., 2020. Sequential Precipitation and Delipidation Enables Efficient Enrichment of Low-Molecular Weight Proteins and Peptides from Human Plasma. *J Proteome Res* 19, 3340–3351. <https://doi.org/10.1021/acs.jproteome.0c00232>.
- Lim, J.-H., Kim, M.-S., Kim, H.-E., Yano, T., Oshima, Y., Aggarwal, K., Goldman, W.E., Silverman, N., Kurata, S., Oh, B.-H., 2006. Structural basis for preferential recognition of diaminopimelic acid-type peptidoglycan by a subset of peptidoglycan

- recognition proteins. *J Biol Chem* 281, 8286–8295. <https://doi.org/10.1074/jbc.M513030200>.
- Limmer, S., Weiler, A., Volkenhoff, A., Babatz, F., Klämbt, C., 2014. The *Drosophila* blood-brain barrier: development and function of a glial endothelium. *Front Neurosci* 8, 365. <https://doi.org/10.3389/fnins.2014.00365>.
- Liu, T., Zhang, L., Joo, D., Sun, S.-C., 2017. NF- κ B signaling in inflammation. *Signal Transduct Target Ther* 2, 17023. <https://doi.org/10.1038/sigtrans.2017.23>.
- Long, X., Colonell, J., Wong, A.M., Singer, R.H., Lionnet, T., 2017. Quantitative mRNA imaging throughout the entire *Drosophila* brain. *Nat Methods* 14, 703–706. <https://doi.org/10.1038/nmeth.4309>.
- Maillet, F., Bischoff, V., Vignal, C., Hoffmann, J., Royet, J., 2008. The *Drosophila* peptidoglycan recognition protein PGRP-LF blocks PGRP-LC and IMD/JNK pathway activation. *Cell Host Microbe* 3, 293–303. <https://doi.org/10.1016/j.chom.2008.04.002>.
- Masuzo, A., Manière, G., Viallat-Lieutaud, A., Avazeri, É., Zugasti, O., Grosjean, Y., Kurrz, C.L., Royet, J., 2019. Peptidoglycan-Dependent NF-Kb Activation in a Small Subset of Brain Octopaminergic Neurons Controls Female Oviposition. *eLife* 8: e50559 <https://doi.org/10.7554/eLife.50559>.
- McFall-Ngai, M., Hadfield, M.G., Bosch, T.C.G., Carey, H.V., Domazet-Lošo, T., Douglas, A.E., Dubilier, N., Eberl, G., Fukami, T., Gilbert, S.F., Hentschel, U., King, N., Kjelleberg, S., Knoll, A.H., Kremer, N., Mazmanian, S.K., Metcalf, J.L., Nealon, K., Pierce, N.E., Rawls, J.F., Reid, A., Ruby, E.G., Rumpho, M., Sanders, J. G., Tautz, D., Wernegreen, J.J., 2013. Animals in a bacterial world, a new imperative for the life sciences. *Proc Natl Acad Sci U S A* 110, 3229–3236. <https://doi.org/10.1073/pnas.1218525110>.
- Meinander, A., Runchel, C., Tenev, T., Chen, L., Kim, C.-H., Ribeiro, P.S., Broemer, M., Leulier, F., Zvelebil, M., Silverman, N., Meier, P., 2012. Ubiquitylation of the initiator caspase DREDD is required for innate immune signalling. *EMBO J* 31, 2770–2783. <https://doi.org/10.1038/emboj.2012.121>.
- Mellroth, P., Steiner, H., 2006. PGRP-SB1: An N-acetylmuramoyl l-alanine amidase with antibacterial activity. *Biochemical and Biophysical Research Communications* 350, 994–999. <https://doi.org/10.1016/j.bbrc.2006.09.139>.
- Michel, T., Reichhart, J.M., Hoffmann, J.A., Royet, J., 2001. *Drosophila* Toll is activated by Gram-positive bacteria through a circulating peptidoglycan recognition protein. *Nature* 414, 756–759. <https://doi.org/10.1038/414756a>.
- Morais, L.H., Schreiber, H.L., Mazmanian, S.K., 2021. The gut microbiota–brain axis in behaviour and brain disorders. *Nat Rev Microbiol* 19, 241–255. <https://doi.org/10.1038/s41579-020-00460-0>.
- Mozzak, M., Szulínska, M., Bogdański, P., 2020. You Are What You Eat—The Relationship between Diet, Microbiota, and Metabolic Disorders—A Review. *Nutrients* 12, 1096. <https://doi.org/10.3390/nu12041096>.
- Myllymäki, H., Rämet, M., 2014. JAK/STAT Pathway in *Drosophila* Immunity. *Scandinavian Journal of Immunology* 79, 377–385. <https://doi.org/10.1111/sji.12170>.
- Myllymäki, H., Valanne, S., Rämet, M., 2014. The *Drosophila* Imd Signaling Pathway. *The Journal of Immunology* 192, 3455–3462. <https://doi.org/10.4049/jimmunol.1303309>.
- Nagpal, J., Cryan, J.F., 2021. Microbiota-brain interactions: Moving toward mechanisms in model organisms. *Neuron* 109, 3930–3953. <https://doi.org/10.1016/j.neuron.2021.09.036>.
- Neyen, C., Poidevin, M., Roussel, A., Lemaître, B., 2012. Tissue- and Ligand-Specific Sensing of Gram-Negative Infection in *Drosophila* by PGRP-LC Isoforms and PGRP-LE. *The Journal of Immunology* 189, 1886–1897. <https://doi.org/10.4049/jimmunol.1201022>.
- Onuma, T., Yamauchi, T., Kosakamoto, H., Kadoguchi, H., Kuraishi, T., Murakami, T., Mori, H., Miura, M., Obata, F., 2023. Recognition of commensal bacterial peptidoglycans defines *Drosophila* gut homeostasis and lifespan. *PLOS Genetics* 19, e1010709.
- Paik, D., Monahan, A., Caffrey, D.R., Elling, R., Goldman, W.E., Silverman, N., 2017. SLC46 family transporters facilitate cytosolic innate immune recognition of monomeric peptidoglycans. *J Immunol* 199, 263–270. <https://doi.org/10.4049/jimmunol.1600409>.
- Paredes, J.C., Welchman, D.P., Poidevin, M., Lemaître, B., 2011. Negative Regulation by Amidase PGRPs Shapes the *Drosophila* Antibacterial Response and Protects the Fly from Innocuous Infection. *Immunity* 35, 770–779. <https://doi.org/10.1016/j.immuni.2011.09.018>.
- Park, J.T., Uehara, T., 2008. How bacteria consume their own exoskeletons (turnover and recycling of cell wall peptidoglycan). *Microbiol Mol Biol Rev* 72:211–227. <https://doi.org/10.1128/MMBR.00027-07> table of contents.
- Phillips, M.D., Thomas, C.M., 2006. Brush border spectrin is required for early endosome recycling in *Drosophila*. *J Cell Sci* 119, 1361–1370. <https://doi.org/10.1242/jcs.02839>.
- Proctor LM, Creasy HH, Fettweis JM, Lloyd-Price J, Mahurkar A, Zhou W, Buck GA, Snyder MP, Strauss JF, Weinstock GM, White O, Huttenhower C, The Integrative HMP (iHMP) Research Network Consortium. 2019. The Integrative Human Microbiome Project. *Nature* 569:641–648. doi:10.1038/s41586-019-1238-8.
- Sampath, V., 2018. Bacterial endotoxin-lipopolysaccharide; structure, function and its role in immunity in vertebrates and invertebrates. *Agriculture and Natural Resources* 52, 115–120. <https://doi.org/10.1016/j.anres.2018.08.002>.
- Sanchez Bosch, P., Makhijani, K., Herboso, L., Gold, K.S., Baginsky, R., Woodcock, K.J., Alexander, B., Kukar, K., Corcoran, S., Jacobs, T., Ouyang, D., Wong, C., Ramond, E. J.V., Rhiner, C., Moreno, E., Lemaître, B., Geissmann, F., Brückner, K., 2019. Adult *Drosophila* Lack Hematopoiesis but Rely on a Blood Cell Reservoir at the Respiratory Epithelia to Relay Infection Signals to Surrounding Tissues. *Dev Cell* 51, 787–803.e5. <https://doi.org/10.1016/j.devcel.2019.10.017>.
- Schirmeier, S., Klämbt, C., 2015. The *Drosophila* blood-brain barrier as interface between neurons and hemolymph. *Mechanisms of Development, Neurovascular Unit* 138, 50–55. <https://doi.org/10.1016/j.mod.2015.06.002>.
- Schleifer, K.H., Kandler, O., 1972. Peptidoglycan types of bacterial cell walls and their taxonomic implications. *Bacteriological Reviews* 36, 407. <https://doi.org/10.1128/br.36.4.407-477.1972>.
- Sorbara, M.T., Philpott, D.J., 2011. Peptidoglycan: a critical activator of the mammalian immune system during infection and homeostasis. *Immunological Reviews* 243, 40–60. <https://doi.org/10.1111/j.1600-065X.2011.01047.x>.
- Stork, T., Engelen, D., Krudewig, A., Silies, M., Bainton, R.J., Klämbt, C., 2008. Organization and Function of the Blood-Brain Barrier in *Drosophila*. *J Neurosci* 28, 587–597. <https://doi.org/10.1523/JNEUROSCI.4367-07.2008>.
- Tosoni, G., Conti, M., Diaz, H.R., 2019. Bacterial peptidoglycans as novel signaling molecules from microbiota to brain. *Curr Opin Pharmacol* 48, 107–113. <https://doi.org/10.1016/j.coph.2019.08.003>.
- Tzou, P., Ohresser, S., Ferrandon, D., Capovilla, M., Reichhart, J.-M., Lemaître, B., Hoffmann, J.A., Imler, J.-L., 2000. Tissue-Specific Inducible Expression of Antimicrobial Peptide Genes in *Drosophila* Surface Epithelia. *Immunity* 13, 737–748. [https://doi.org/10.1016/S1074-7613\(00\)00072-8](https://doi.org/10.1016/S1074-7613(00)00072-8).
- Vance, R.E., Isberg, R.R., Portnoy, D.A., 2009. Patterns of pathogenesis: discrimination of pathogenic and non-pathogenic microbes by the innate immune system. *Cell Host Microbe* 6, 10–21. <https://doi.org/10.1016/j.chom.2009.06.007>.
- Visser, L., Jan de Heer, H., Boven, L.A., van Riel, D., van Meurs, M., Melief, M.-J., Zähringer, U., van Strijp, J., Lambrecht, B.N., Nieuwenhuis, E.E., Laman, J.D., 2005. Proinflammatory bacterial peptidoglycan as a cofactor for the development of central nervous system autoimmune disease. *J Immunol* 174, 808–816. <https://doi.org/10.4049/jimmunol.174.2.808>.
- Volkenhoff, A., Weiler, A., Letzel, M., Stehling, M., Klämbt, C., Schirmeier, S., 2015. Glial Glycolysis Is Essential for Neuronal Survival in *Drosophila*. *Cell Metab* 22, 437–447. <https://doi.org/10.1016/j.cmet.2015.07.006>.
- Vollmer, W., Blant, D., De Pedro, M.A., 2008. Peptidoglycan structure and architecture. *FEMS Microbiology Reviews* 32, 149–167. <https://doi.org/10.1111/j.1574-6976.2007.00094.x>.
- Weiler, A., Volkenhoff, A., Hertenstein, H., Schirmeier, S., 2017. Metabolite transport across the mammalian and insect brain diffusion barriers. *Neurobiol Dis* 107, 15–31. <https://doi.org/10.1016/j.nbd.2017.02.008>.
- Wheeler, R., Bastos, P.A.D., Disson, O., Rifflet, A., Gabanyi, I., Spielbauer, J., Bérard, M., Lecuit, M., Boneca, I.G., 2023. Microbiota-induced active translocation of peptidoglycan across the intestinal barrier dictates its within-host dissemination. *Proc Natl Acad Sci U S A* 120. <https://doi.org/10.1073/pnas.2209936120> e2209936120.
- Winkler, B., Funke, D., Benmimoun, B., Spéder, P., Rey, S., Logan, M.A., Klämbt, C., 2021. Brain inflammation triggers macrophage invasion across the blood-brain barrier in *Drosophila* during pupal stages. *Sci Adv* 7:eabh0050. <https://doi.org/10.1126/sciadv.abh0050>.
- Wolf, A.J., Underhill, D.M., 2018. Peptidoglycan recognition by the innate immune system. *Nat Rev Immunol* 18, 243–254. <https://doi.org/10.1038/nri.2017.136>.
- Yildirim, K., Petri, J., Kottmeier, R., Klämbt, C., 2019. *Drosophila* glia: Few cell types and many conserved functions. *Glia* 67, 5–26. <https://doi.org/10.1002/glia.23459>.
- Younes, S., Al-Sulaiti, A., Nasser, E.A.A., Najjar, H., Kamareddine, L., 2020. *Drosophila* as a Model Organism in Host-Pathogen Interaction Studies. *Frontiers in Cellular and Infection Microbiology* 10. <https://doi.org/10.3389/fcimb.2020.00214>.
- Zaidman-Rémy, A., Hervé, M., Poidevin, M., Pili-Floury, S., Kim, M.-S., Blant, D., Oh, B.-H., Ueda, R., Mengin-Lecreulx, D., Lemaître, B., 2006. The *Drosophila* amidase PGRP-LB modulates the immune response to bacterial infection. *Immunity* 24, 463–473. <https://doi.org/10.1016/j.immuni.2006.02.012>.
- Zaidman-Rémy, A., Poidevin, M., Hervé, M., Welchman, D.P., Paredes, J.C., Fahlander, C., Steiner, H., Mengin-Lecreulx, D., Lemaître, B., 2011. *Drosophila* Immunity: Analysis of PGRP-SB1 Expression, Enzymatic Activity and Function. *PLOS ONE* 6, e17231.
- Zugasti, O., Vagnon, R., Royet, J., 2020. Gut bacteria-derived peptidoglycan induces a metabolic syndrome-like phenotype via NF- κ B-dependent insulin/PI3K signaling reduction in *Drosophila* renal system. *Sci Rep* 10, 14097. <https://doi.org/10.1038/s41598-020-70455-7>.